

Synthesis and Kinetic Evaluation of Cyclophostin and Cyclipostins Phosphonate Analogs As Selective and Potent Inhibitors of Microbial Lipases

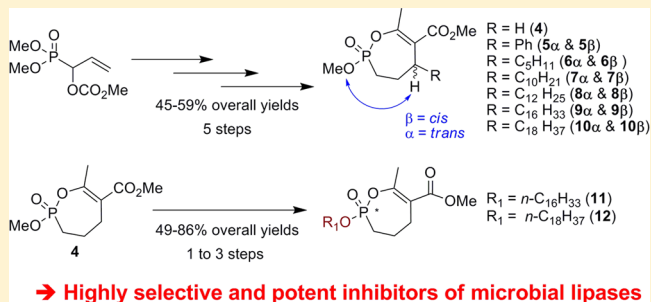
Vanessa Point,^{†,§} Raj K. Malla,^{‡,§} Sadia Diomande,[†] Benjamin P. Martin,[‡] Vincent Delorme,[†] Frederic Carriere,[†] Stephane Canaan,[†] Nigam P. Rath,[‡] Christopher D. Spilling,^{*,‡} and Jean-François Cavalier^{*,†}

[†]CNRS - Aix-Marseille Université, Enzymologie Interfaciale et Physiologie de la Lipolyse, UMR 7282, 31 chemin Joseph Aiguier, 13402 Marseille cedex 20, France

[‡]Department of Chemistry and Biochemistry, University of Missouri—St. Louis, 1 University Boulevard, St. Louis, Missouri 63121, United States

Supporting Information

ABSTRACT: A new series of customizable diastereomeric *cis*- and *trans*-monocyclic enol-phosphonate analogs to Cyclophostin and Cyclipostins were synthesized. Their potencies and mechanisms of inhibition toward six representative lipolytic enzymes belonging to distinct lipase families were examined. With mammalian gastric and pancreatic lipases no inhibition occurred with any of the compounds tested. Conversely, *Fusarium solani* Cutinase and lipases from *Mycobacterium tuberculosis* (Rv0183 and LipY) were all fully inactivated. The best inhibitors displayed a *cis* conformation (H and OMe) and exhibited higher inhibitory activities than the lipase inhibitor Orlistat toward the same enzymes. Our results have revealed that chemical group at the γ -carbon of the phosphonate ring strongly impacts the inhibitory efficiency, leading to a significant improvement in selectivity toward a target lipase over another. The powerful and selective inhibition of microbial (fungal and mycobacterial) lipases suggests that these seven-membered monocyclic enol-phosphonates should provide useful leads for the development of novel and highly selective antimicrobial agents.



INTRODUCTION

Lipases and their inhibitors have potential applications in the fields of chemistry,¹ biotechnology,² and medicine. In the latter domain, for instance, inhibiting digestive lipases to reduce fat absorption has become the main pharmacological approach to the treatment of obesity during the past decade.³ The best example is the FDA-approved antiobesity drug Orlistat (marketed as Xenical by Roche and Alli by GlaxoSmithKline), which reacts with the nucleophilic serine residue from the catalytic triad of pancreatic and gastric lipases and inhibits these enzymes within the gastrointestinal tract.^{4,5} Orlistat is also known to inhibit various other enzymes, like fatty acid synthase,⁶ providing this compound with potential applications in the treatment of Alzheimer's disease,⁷ type II diabetes,⁸ and antitumoral⁶ and antimycobacterial^{9–11} activities. However, this lack of selectivity could also lead to undesirable side effects, which might affect its current clinical use.

In this context, designing and synthesizing selective inhibitors of various animal and microbial lipases represent attractive and useful probes to reveal the catalytic mechanisms of these lipases, and especially to better understand specific enzyme–substrate interactions.¹² Such inhibitors also represent

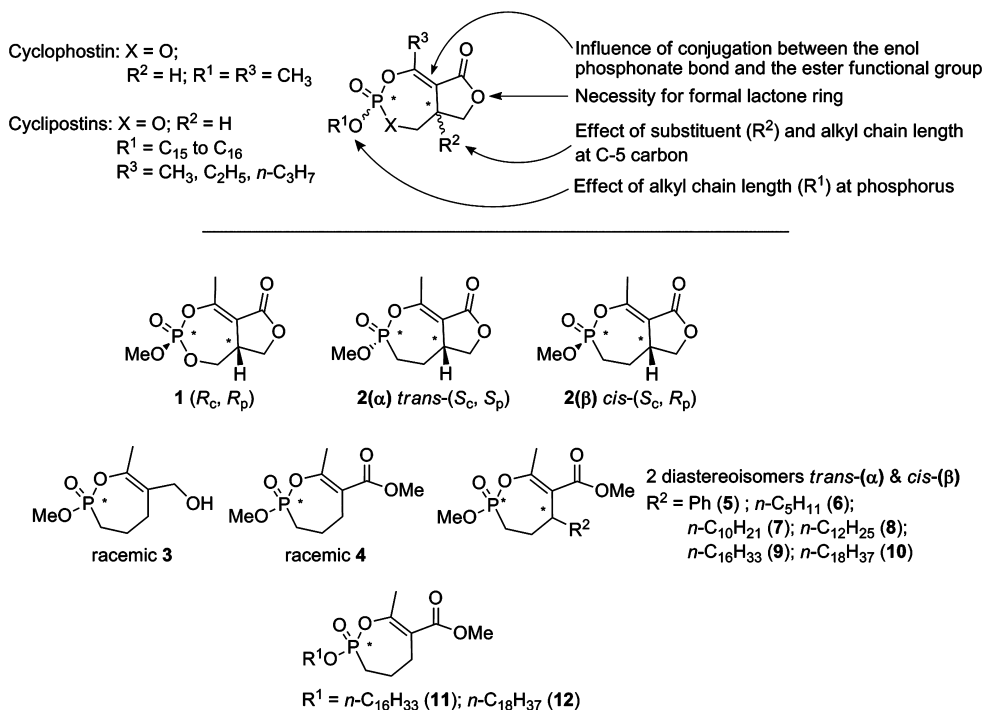
attractive leads for developing specific treatments toward various organisms involving lipolytic enzymes as essential metabolic enzymes or virulence factors.^{13,14} Phosphonate analogs of biologically active phosphates have been shown to be extremely useful tools in investigating mechanistic details of various enzymatic systems.^{15,16} Their success is usually attributed to the nonhydrolyzability of a P–C bond (phosphonate analog) when compared to the P–O bond of the corresponding phosphate leading to an enhanced compound lifetime *in vivo*.^{17,18} Moreover, phosphonates are known to mimic in both their charge distribution and geometry the first transition state occurring during enzymatic carboxylester hydrolysis, with the formation of an irreversible covalent bond between the nucleophilic O γ of the active site serine and the phosphorus atom.¹⁹

Cyclophostin (Scheme 1), a bicyclic enol-phosphate isolated from a fermentation solution of *Streptomyces lavendulae* (strain NK901093),²⁰ was identified as an irreversible inhibitor of acetylcholinesterase (AChE) with IC₅₀ values in the nanomolar

Received: September 6, 2012

Published: October 24, 2012

Scheme 1. Rationale for Synthesis of Cyclophostin and Cyclipostins Analogs, And Related Structures Investigated: Cyclophostin Molecule (1)²¹ and Phosphonate Analogs (2);¹⁵ Monocyclic Phosphonate Analogs to Either Cyclophostin (3–4,¹⁶ 5–10) or Cyclipostins (11–12)



range.^{16,20,21} The unusual bicyclic enol-phosphate moiety is also found in a second family of structurally related natural products, named the Cyclipostins²² (Scheme 1). The Cyclipostins possess a core structure similar to that of Cyclophostin but are phosphate esters of long chain lipophilic alcohols of various lengths and structures. All identified Cyclipostins have been described to be potent inhibitors of hormone-sensitive lipase (HSL)²² and have also been reported to inhibit the growth of various mycobacteria including *Mycobacterium smegmatis*, *Mycobacterium phlei*, *Nocardia abscessus*, and *Corynebacterium diphtheriae*.²³ The minimum inhibitory concentrations (MICs) obtained were similar or even lower than those of the well-known antibiotics Rifampicin or Penicillin G. These recent results strongly suggest that Cyclophostin and Cyclipostins compounds can inhibit serine hydrolases produced by these organisms, including mycobacterial lipases.

In the present article, we report the synthesis and first mechanistic study of a new series of cyclic enol phosphonate analogs of both Cyclophostin and Cyclipostins (Scheme 1) as potential inhibitors of lipases. Three mammalian digestive lipases (human pancreatic lipase, HPL; dog gastric lipase, DGL; and guinea pig pancreatic lipase-related protein 2, GPLRP2) and three microbial lipases (*Fusarium solani* Cutinase, *Mycobacterium tuberculosis* Rv0183 and LipY) were chosen as representative enzyme targets. HPL and DGL, the main lipases involved in the digestion of dietary lipids, are *sn*-1,3-regioselective and *sn*-3-stereoselective lipases, respectively, acting on both triacylglycerols and diacylglycerols.²⁴ GPLRP2 belongs to the pancreatic lipase gene family,²⁵ but differs from HPL by its kinetic and structural properties.²⁶ More precisely, the lid domain controlling the access to the active site, as in the case of HPL and DGL,²⁷ is missing in GPLRP2 and its catalytic serine is therefore easily accessible to the solvent.²⁵ GPLRP2

exhibits lipase, phospholipase A1, and galactolipase activities,^{28–30} and its main physiological function is the hydrolysis of dietary galactolipids²⁹ and phospholipids.²⁵ Among the three microbial lipases investigated, Cutinase is able to hydrolyze a wide range of substrates (fatty acid esters, triacylglycerols, and phospholipids) and possesses, like GPLRP2, the advantage to exhibit an active site always accessible to the solvent.^{31–33} *Mycobacterium tuberculosis* Rv0183 is a monoglyceride lipase implicated in the architecture of the membrane and in the degradation of extracellular monoacylglycerols,^{14,34,35} while LipY is a triacylglycerol lipase belonging to the HSL family, involved in triacylglycerol degradation during persistence³⁶ and in host lipid degradation during reactivation of the bacteria.³⁷ Both LipY and Rv0183, which may contribute to the growth and pathogenicity of *Mycobacterium tuberculosis*, therefore appear as potential drug targets against tuberculosis.

These six lipases were then chosen as representative models belonging to different lipase families (Table 1). They have distinct structural properties (with or without a lid controlling the access to the active site for instance) and display various substrate specificities. Such diversity, covering a wide range of lipolytic enzymes, will then allow us to access structure–activity relationships between these targeted enzymes and the diastereoisomeric cyclic enol-phosphonate inhibitors analogous to Cyclipostins and Cyclophostin.

In this context, the inhibitory power and selectivity of this new series of organophosphorous compounds have been evaluated on the basis of the following structural properties: (1) effect of removal of conjugation between the enol-phosphonate bond and the ester functional group; (2) requirement of the formal lactone ring; (3) effect of substituent R² at the C-5 carbon atom; and (4) effect of substituent R¹ at the phosphorus atom (Scheme 1). To reach this goal, new synthetic routes were developed in order to easily provide a

Table 1. Biochemical Properties of the Six Lipases Tested

Enzyme	Lipase gene family	Presence of a "lid"	Main substrates
DGL	Acid lipase	Yes (PDB ID: 1K8Q) ^a	Triacylglycerols Diacylglycerols
HPL	Pancreatic lipase	Yes (PDB ID: 1LPB) ^b	Triacylglycerols Diacylglycerols
GPLRP2	Pancreatic lipase	No (PDB ID: 1GPL) ^c	Triacylglycerols Phospholipids Galactolipids
Cutinase	Fungal lipase	No (PDB ID: 1XZL) ^d	Cutin Triacylglycerols Phospholipids Galactolipids
Rv0183	Monoglyceride lipase	Structural data unavailable	Monoacylglycerols
LipY	Hormone-sensitive lipase	Structural data unavailable	Triacylglycerols

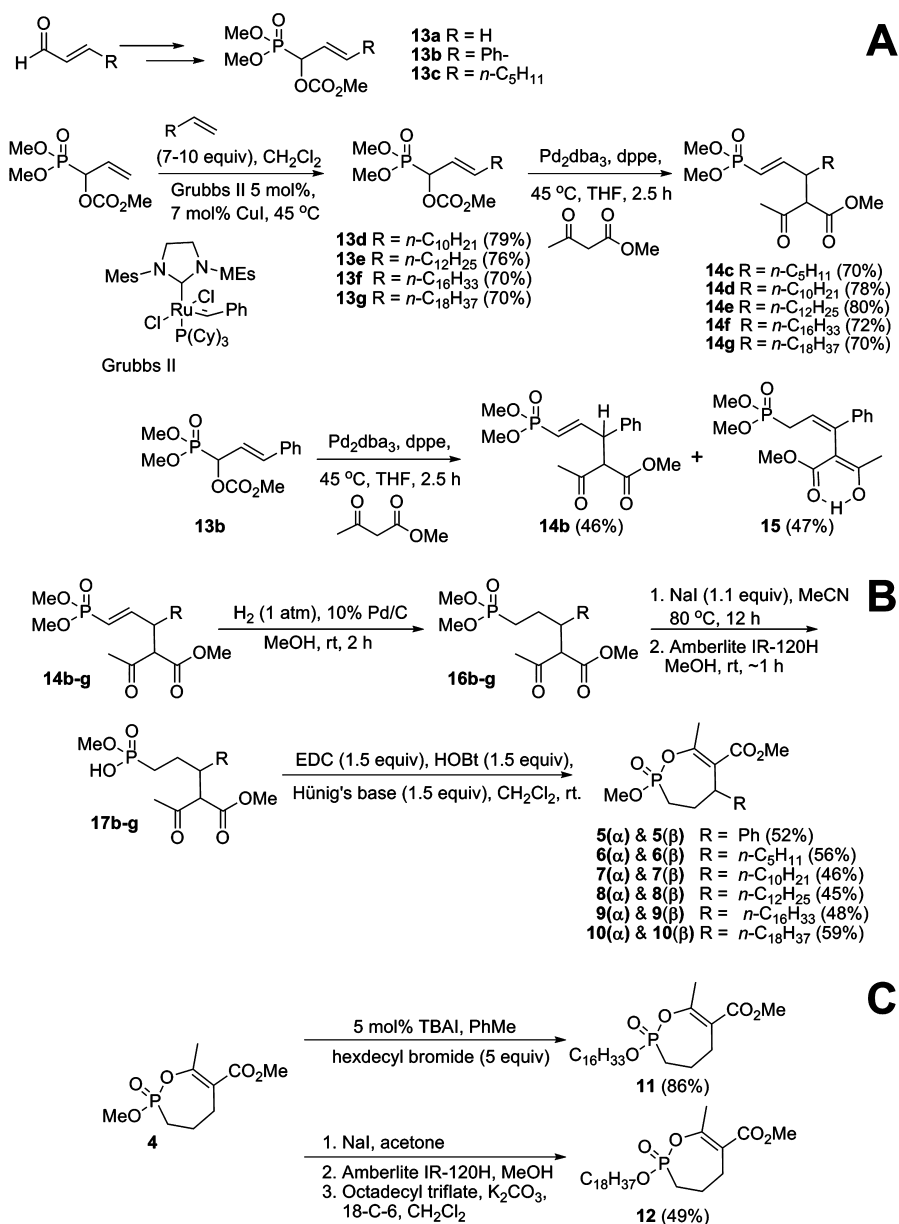
^aSee ref 44. ^bSee ref 45. ^cSee ref 25. ^dSee ref 31.

library of enol-phosphonate compounds bearing different chemical groups.

RESULTS

Synthesis of Cyclophostin and Cyclophostins Phosphonate Analogs. The syntheses of racemic Cyclophostin 1,²¹ racemic bicyclic phosphonate analogs 2(α)/2(β),¹⁵ and unsubstituted monocyclic analogs 3 and 4¹⁶ have already been reported. In general, the methods employed in the synthesis of 2(α)/2(β) and 4 were adapted to the synthesis of the novel substituted monocyclic phosphonate analogs 5–10. The precursor carbonates 13a–13c were prepared following literature methods³⁸ (Scheme 2A). Additional carbonates 13d–13g were prepared by the cross metathesis reaction of the parent acrolein-derived carbonate 13a with terminal alkenes using Grubbs' second generation catalyst with copper(I) iodide as the cocatalyst.^{38,39} The carbonates 13d–13g were formed in good yields (70–79%) as a mixture of *E* and *Z* isomers in ratios

Scheme 2. Synthesis of Novel Monocyclic Enol-Phosphonate Analogs of Either Cyclophostin (5–10) or Cyclophostins (11–12)



varying from 9:1 to 14:1. Palladium(0)-catalyzed reactions of the carbonates **13c–13g** with methyl acetoacetate gave the vinyl phosphonates **14c–g** (Scheme 2A) in good yields (70–80%). The products were formed as diastereoisomeric mixtures, but with exclusively *E* alkene geometry. However, the reaction of carbonate **13b** produced both the vinyl phosphonate **14b** and the allyl phosphonate **15**, which is the result of the migration of the double bond into conjugation with the phenyl group. Interestingly, spectroscopic analysis (NMR and IR) and X-ray crystallography showed that the allyl phosphonate **15** exists predominantly in the enol-form of β -keto ester. Both vinyl **14b** and allyl phosphonates **15** were taken on to the next step since, after hydrogenation, they should yield the same alkyl phosphonate.

The treatment of a methanolic solution of the vinyl phosphonates **14b–g** (or **15**) with hydrogen gas over 10% palladium on carbon gave saturated phosphonates **16a–g** in quantitative yields (Scheme 2B). As expected, hydrogenation of either **14** or **15** gave the saturated phosphonate **16b**. The phosphonates **16b–16g** were monodemethylated using sodium iodide (1.1 equiv) in refluxing acetonitrile to give the corresponding sodium salts, which were subsequently converted to monophosphonic acids **17a–g** by treatment with Amberlite IR-120H resin in methanol. The monophosphonic acids **17a–g** were cyclized, without further purification, using a combination of EDC, HOBT, and Hünig's base (*i*-Pr₂NEt) to give the substituted monocyclic phosphonates **5–10** as diastereoisomeric mixtures in 45–59% yields over the three steps. As previously demonstrated in the synthesis of the racemic bicyclic phosphonate analogs of Cyclophostin **2(α)** and **2(β)**,¹⁵ compounds **5** to **10** were best described by the relationship between the OMe on phosphorus and the H-substituent on the C-5 carbon atom as being either in a *trans* (α -isomer) or *cis* (β -isomer) relationship. The two racemic diastereoisomers (α and β) were further separated by careful silica gel column chromatography (Scheme 2B). A single crystal X-ray diffraction structure of **10(α)** was further obtained at an edge resolution of ~ 0.97 Å (Tables S1 to S5) thus confirming these stereochemical assignments (*trans-α* and *cis-β*). As shown in Figure 1, the obtained structure clearly exhibits a *trans* relationship between the methoxy (numbered O2–C25) and the hydrogen atom located on the carbon numbered C3.

The initial approach to forming long chain phosphonate esters (Scheme 2C) from the monocyclic phosphonate **4** involved demethylation and then realkylation in three separate reaction steps. Thus, the phosphonate **4** was treated with NaI in acetone to give the sodium salt, which was protonated by treatment with Amberlite IR-120H in methanol. The phosphonic acid was then realkylated using potassium carbonate, 18-Crown-6, and octadecyl triflate⁴⁰ to give phosphonate **12** in 49% yield over three steps. However, we have discovered more recently that a *trans*-esterification reaction of the phosphonate methyl ester **4** (and others) could be performed in a single pot reaction.²¹ The phosphonate **4** was then treated with a 5-fold excess of hexadecyl bromide in toluene with a catalytic amount of *n*Bu₄NI (TBAI) (5 mol %) leading to the hexadecyl phosphonate **11** in 86% yields. Final products **1–12** were fully analyzed and characterized by NMR, HRMS, and HPLC.

Lipase Inhibition. The 18 new chiral organophosphorus compounds synthesized (*i.e.*, compounds **1**, **3** to **5**, **11** and **12**, as well as *trans-α* and *cis-β* isomers of **2** and **6** to **10**; Scheme 1) were further tested for their inhibitory activity

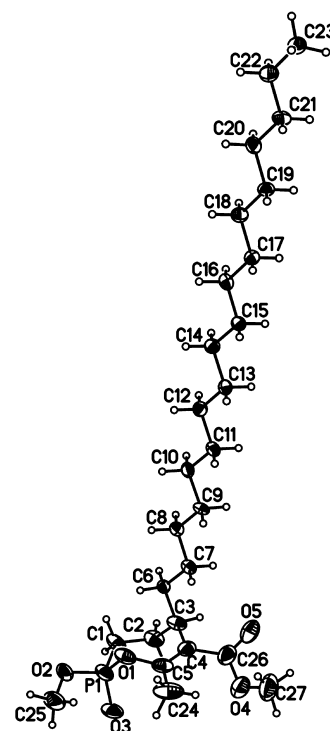


Figure 1. Projection view of **10(α)** with 30% thermal ellipsoids (disorder atoms omitted for clarity). This crystal structure has been deposited at the Cambridge Crystallographic Data Centre and allocated the deposition number CCDC 873939.

toward HPL, DGL, GPLRP2, Cutinase, Rv0183, and LipY. The pH-stat technique⁴¹ was used to measure lipase activities and quantify the inhibitory power, defined here as the inhibitor molar excess leading to 50% lipase inhibition (x_{150} value).⁴² The lipase stereopreference was also assessed through the Diastereoselectivity Index (DI)⁴³ between the two diastereoisomers *trans-α* and *cis-β* as defined in eq 1 (see Experimental Section).

Inhibition Results Using Cyclic Enol-Phosphorus Compounds. A significant inhibition was obtained with the three microbial lipases tested (Table 2). Cutinase was strongly inactivated by most of the organophosphorus compounds, and the efficiency of the inhibition was found to be dependent on the chemical structure of each inhibitor. First, synthetic racemic Cyclophostin **1** ($x_{150} = 0.96$) was 4- to 10-fold more potent than its two homologous phosphonates **2(α)** ($x_{150} = 4.49$) and **2(β)** ($x_{150} = 8.77$). With these two latter compounds, one can also notice that Cutinase exhibited a slight stereopreference for the *trans* isomer **2(α)** (DI = 32.3%). Regarding the monocyclic enol-phosphonates analogous to Cyclophostin molecules, compounds **3** and **5**, bearing respectively an alcohol instead of an ester function and a phenyl group at the C-5 position of the oxaphosphopine cycle, did not inhibit Cutinase. The following classification based on the decreasing inhibitory potency was then obtained: **10(β)** ($x_{150} = 1.18$) > **4** ($x_{150} = 1.39$) \cong **6(β)** ($x_{150} = 1.42$) \geq **7(β)** ($x_{150} = 1.98$) \cong **8(β)** ($x_{150} = 2.00$) > **9(β)** ($x_{150} = 2.54$). In all cases x_{150} values were indicative of a very potent inhibition. In addition, Cutinase showed a strong stereopreference for the (β) isomers having a *cis* conformation. The higher diastereoselectivity (DI > 70.0%) was then found for compounds **6(β)**, **7(β)**, and **10(β)** bearing C5, C10, and C16 aliphatic alkyl chains, respectively. Finally, the Cyclophostin analogs **11** ($x_{150} = 0.56$) and **12** ($x_{150} = 0.95$) as

Table 2. Inhibition of Cutinase, Rv0183 and LipY by Cyclic Enol-Phosphorous Compounds and Orlistat after 30-min Incubation Period^a

compd	Cutinase		Rv0183		LipY	
	x_{150}	DI	x_{150}	DI	x_{150}	DI
1	0.96	–	5.22	–	>100	–
2(α)	4.49	32.3%	41.6	1.9%	>100	NA
2(β)	8.77	–	43.2	–	>100	–
3	>100	–	NI	–	NI	–
4	1.39	–	30.5	–	>100	–
5	>100	–	16.2	–	NI	–
6(α)	26.2	89.7%	3.79	16.7%	>100	NA
6(β)	1.42	–	2.70	–	>100	–
7(α)	14.6	–	3.57	–	25.8	–
7(β)	1.98	76.2%	1.13	51.9%	2.81	80.3%
8(α)	3.63	–	2.44	–	6.14	–
8(β)	2.00	29.0%	5.23	36.3%	3.46	28.0%
9(α)	4.43	–	>100	>97.0%	3.47	–
9(β)	2.54	27.2%	1.32	–	0.60	70.5%
10(α)	7.26	–	>100	–	7.47	–
10(β)	1.18	72.1%	3.15	>93.0%	0.77	81.3%
11	0.56	–	NI	–	0.83	–
12	0.95	–	NI	–	0.59	–
Orlistat	2.52	–	>200	–	7.07	–

^a x_{150} values were determined as described in Experimental Section. Diastereoselectivity Index (DI) between *trans*-(α) and *cis*-(β) isomers was calculated for compounds 2 and 6 to 10 using eq 1. Results are expressed as mean values of at least two independent assays (CV% < 5.0%). NA = not applicable. NI = no significant inhibition observed.

well as Cyclophostin 1 ($x_{150} = 0.96$) were found to be the best inhibitors of Cutinase. Based on the absence of inhibition observed with compounds 3 and 5 ($x_{150} > 100$), a free or cyclic (lactone) ester group appears to therefore be required to provide the enol-phosphonates with inhibitory activity.

Concerning Rv0183, the monoglyceride lipase from *Mycobacterium tuberculosis*,³⁴ Cyclophostin 1 displayed a x_{150} value of 5.22 which was nearly 8-fold lower than that of its homologous phosphonates 2(α , β) (mean $x_{150} = 42.4 \pm 0.8$). Low lipophilic compounds 2(α , β), 4, and 5 also exhibited rather weak inhibitory power with x_{150} values ranging from 16.2 to 43.2. Compound 3, which has an alcohol instead of an ester function, was completely inactive toward this lipase. In contrast, the more lipophilic enol-phosphonates 6 to 10 strongly inhibited Rv0183, with x_{150} values in the 1.1 to 5.2 range. Surprisingly, Cyclophostins analogs 11 and 12 were not inhibitors of Rv0183, suggesting that the positioning of the C16–C18 alkyl chains on the phosphorus atom may be responsible for this lack of inhibition. Rv0183 displayed a low diastereoselectivity (DI = 17–52%) between *trans*-(α) and *cis*-(β) isomers when using compounds 6 to 8, suggesting that both conformations where similarly recognized when short (C5) and medium (C10–C12) alkyl chain lengths were present at the C-5 carbon atom. By contrast, only *cis*-(β) isomers of compounds 9 and 10 bearing long (C16–C18) alkyl chains were found to be active against the Rv0183 monoglyceride lipase. These findings highlight the fact that the ester function is necessary but not sufficient to inhibit Rv0183. This monoglyceride lipase therefore displayed a strong chemopreference for lipophilic Cyclophostin enol-phosphonate analogs and a high stereopreference for the *cis*-(β) isomers bearing long C16–C18 alkyl chain length. The best inhibitors

were found to be the Cyclophostin enol-phosphonate analogs 7(β) ($x_{150} = 1.13$) and 9(β) ($x_{150} = 1.32$).

Compounds 1, 2, 4, and 6 exhibited very weak inhibitory properties toward LipY, with 14% to 36% inhibition at a high x_1 value of 40. No inhibition of LipY was obtained with compounds 3 and 5. Conversely, LipY displayed an unambiguous chemopreference for the most lipophilic phosphonates 7(β) ($x_{150} = 2.81$), 8(β) ($x_{150} = 3.46$), 9(β) ($x_{150} = 0.60$), and 10(β) ($x_{150} = 0.77$), all bearing medium to long alkyl chain lengths. Moreover, and as expected for a member of the HSL family,²² LipY was strongly inactivated by the two monocyclic enol-phosphonates 11 ($x_{150} = 0.83$) and 12 ($x_{150} = 0.59$) analogous to Cyclophostins. Interestingly, no significant differences in x_{150} values were observed between the Cyclophostin analogs 9(β) and 10(β) (mean $x_{150} = 0.69 \pm 0.08$), and phosphonates 11 and 12 (mean $x_{150} = 0.71 \pm 0.12$). Such a result suggests that the presence of a long C16–C18 lipophilic alkyl chain is essential for high inhibition to take place, whatever its positioning: either on the C-5 carbon atom of the oxaphosphopine cycle (*i.e.*, in 9(β) and 10(β)) or on the phosphorus atom (*i.e.*, in 11 and 12). As in the case of Cutinase and Rv0183, LipY exhibited a high diastereoselectivity ($28.0 \leq DI \leq 81.3\%$) for the *cis*-(β) isomers. The best inhibitors of LipY were then Cyclophostin analogs 11 ($x_{150} = 0.83$) and 12 ($x_{150} = 0.59$) as well as Cyclophostin analogs 9(β) ($x_{150} = 0.60$) and 10(β) ($x_{150} = 0.77$).

The influence of the incubation time on the levels of inhibition of Cutinase, Rv0183, and LipY by inhibitors 1, 7(β), and 11 was then investigated. As depicted in Figure 2, the

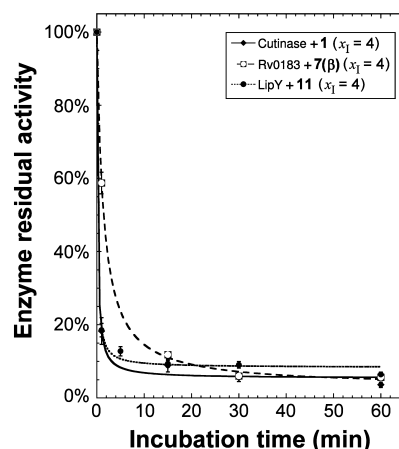


Figure 2. Effect of the incubation time on the inhibition level of Cutinase (\blacklozenge), Rv0183 (\square), and LipY (\bullet) by compounds 1, 7(β), and 11, respectively. Each enzyme was preincubated with the corresponding phosphonate compound at a fixed inhibitor molar excess $x_1 = 4$, and the residual activity was measured over a 60-min period at various time intervals using the pH-stat technique. Results are expressed as mean values of at least two independent assays (CV% < 5.0%).

residual activity of all three enzymes decreased rapidly and reached a plateau value at around 6.0% residual lipase activity after approximately 30 min of incubation. From these inhibition curves, the values of the half-inactivation time ($t_{1/2}$) were determined and found to be 0.18 min for 1 acting on Cutinase, 1.44 min for 7(β) acting on Rv0183, and 0.16 min for 11 acting on LipY. Such values thus reflect an extremely high rate of inhibition of each lipase by the corresponding phosphonate compounds.

In order to compare the inhibitory activity of these organophosphorous compounds with that of Orlistat, the same kinetic parameters were also measured with this inhibitor and each of the tested lipases. The inhibitory effects of Orlistat toward Cutinase ($x_{150} = 2.52$), LipY ($x_{150} = 7.07$), and Rv0183 ($x_{150} > 200$) was found to be 2.6- to 177-fold lower than that of compounds **1** ($x_{150} = 0.96$), **11** ($x_{150} = 0.83$), and **7**(β) ($x_{150} = 1.13$) acting on the same lipases, respectively. Conversely, while Orlistat is a potent inhibitor of mammalian lipases, *i.e.* HPL ($x_{150} = 18.4$), GPLRP2 ($x_{150} = 0.53$), and DGL ($x_{150} = 5.60$), these lipases are not inhibited by all the enol-phosphorus compounds tested, even by using a high inhibitor molar excess ($x_1 = 200$) and after 2 h of incubation. To further investigate such an absence of inhibition experimentally observed with these cyclic enol-phosphorus compounds, *in silico* molecular docking experiments were conducted on **7**(β) with the reported crystal structures of DGL,⁴⁴ HPL,⁴⁵ and GPLRP2²⁵ (Figure 3). In all cases, the best scoring positions obtained (*i.e.* lowest energy complex) showed that the reactive oxaphospe-

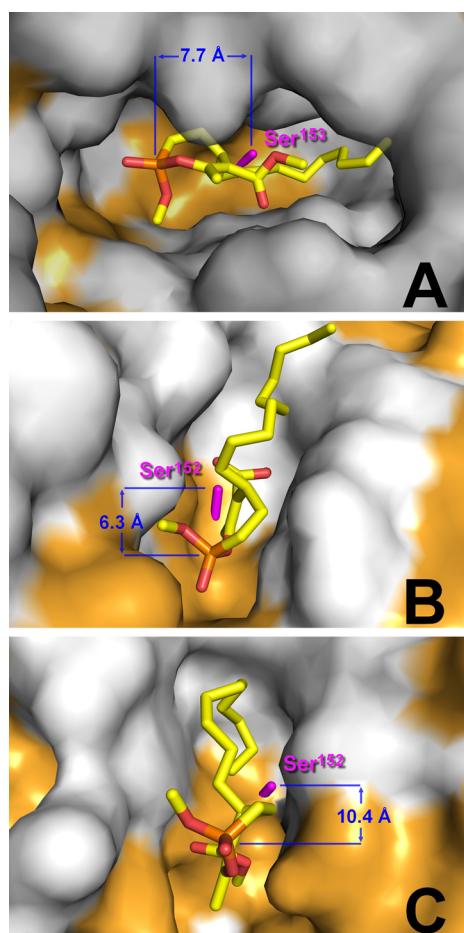


Figure 3. *In silico* molecular docking of compound **7**(β) into crystallographic structures of (A) DGL (PDB: 1K8Q), (B) HPL (PDB: 1LPB), and (C) GPLRP2 (PDB: 1GPL) in a van der Waals surface representation. Hydrophobic residues (alanine, leucine, isoleucine, valine, tryptophan, tyrosine, phenylalanine, proline, and methionine) are highlighted in white. The side chain of the catalytic serine residue is shown as sticks and colored in magenta. Compound **7**(β) is represented in atom color-code sticks (carbon, yellow; phosphorus, orange; oxygen, red). Structures were drawn using the PyMOL Molecular Graphics System (Version 1.3, Schrödinger, LLC). The [Ser-O γ /P] calculated distances are indicated in blue.

pine ring adopted a nonproductive orientation. The phosphorus atom of **7**(β) was indeed found in an opposite and unfavorable position preventing the occurrence of any reactions with the catalytic serine ([Ser-O γ /P] distances >6.0 Å) and thus the formation of a covalent bond.

Mass Spectrometry Analysis of Inhibitor-Modified Enzymes. To investigate whether the inhibition with cyclic enol-phosphonates occurring with microbial lipases is due to the formation of a covalent bond with the catalytic serine, mass spectrometry analyses were further conducted on Cutinase, Rv0183, and LipY inhibited by compounds **4**, **7**(β), and **11**, respectively. Samples of the lipase–inhibitor complexes were then subjected to MALDI-TOF mass spectrometry analyses. The obtained m/z mass values are summarized in Table 3.

Table 3. Mass Spectrometry Analysis of Lipases Inhibited by Monocyclic Enol-Phosphonate Inhibitors^a

species	m/z native lipase, (1)	m/z inhibited lipase, (2)	mass modifications, (2)–(1)
Cutinase	22 187.9 Da	22 420.8 Da	+232.9 Da
Rv0183	30 177.4 Da	30 494.2 Da	+376.8 Da
LipY	47 145.6 Da	47 589.4 Da	+443.8 Da

^aCutinase, Rv0183 and LipY were preincubated for 30 min at 25 °C with compound **4** (M_w , 234.2 Da), **7**(β) (M_w , 374.4 Da), and **11** (M_w , 444.3 Da) respectively, at a x_1 value of 40, prior to MALDI-TOF mass spectrometry analysis.

In the presence of an inhibitor, a shift in the molecular mass of each inhibited protein was observed, corresponding to the molecular mass of the inhibitor and reflecting the covalent binding of **4** (M_w , 234.2 Da) to Cutinase, of **7**(β) (M_w , 374.4 Da) to Rv0183, as well as of **11** (M_w , 444.3 Da) to LipY. Moreover, in order to confirm the mechanism of action of these phosphonate compounds and consequently their specific covalent binding *via* a nucleophilic attack of the catalytic serine residue to the phosphorus center, as initially argued with human AChE,¹⁶ tryptic digestion of the Cutinase-**4** complex was performed. The peptide mass fingerprint (PMF)⁴⁶ was then established by MALDI-TOF mass spectrometry. Peptide C¹⁰⁹-R¹³⁸ (C¹⁰⁹PDATLIAGGYS¹²⁰QGAALAAASIEDLDSAIR¹³⁸) containing the catalytic Ser¹²⁰ residue was detected in the native Cutinase as a multiplet at a molecular mass of around 2977.5 Da (Figure 4A). This catalytic peptide appeared concomitantly with a second multiplet peptide (V¹⁶⁹-R¹⁹⁶) detected at a molecular mass of around 2974.5 Da. When Cutinase was complexed with compound **4**, a mass increase of +234.14 Da was obtained for the catalytic peptide only (Figure 4B), while multiplet peptide V¹⁶⁹-R¹⁹⁶ remained unchanged. The disappearance of 2977.5 Da peptide in the inhibited lipase followed by the appearance of a new one at m/z of 3211.7 Da confirmed that a covalent bond had been formed between the enol-phosphonate **4** and the catalytic serine residue of Cutinase, in accordance with the reaction mechanism depicted in Figure 4C.

DISCUSSION

Cyclophostin and the Cyclophostins are known to be very potent natural organophosphate-based inhibitors of AChE²⁰ and HSL,²² respectively. Variation of the nature of the alkyl group at the phosphate center, methyl vs long lipophilic alkyl groups, leads to a dramatic switch of the enzyme selectivity by these organophosphates. This particular fact provides a unique

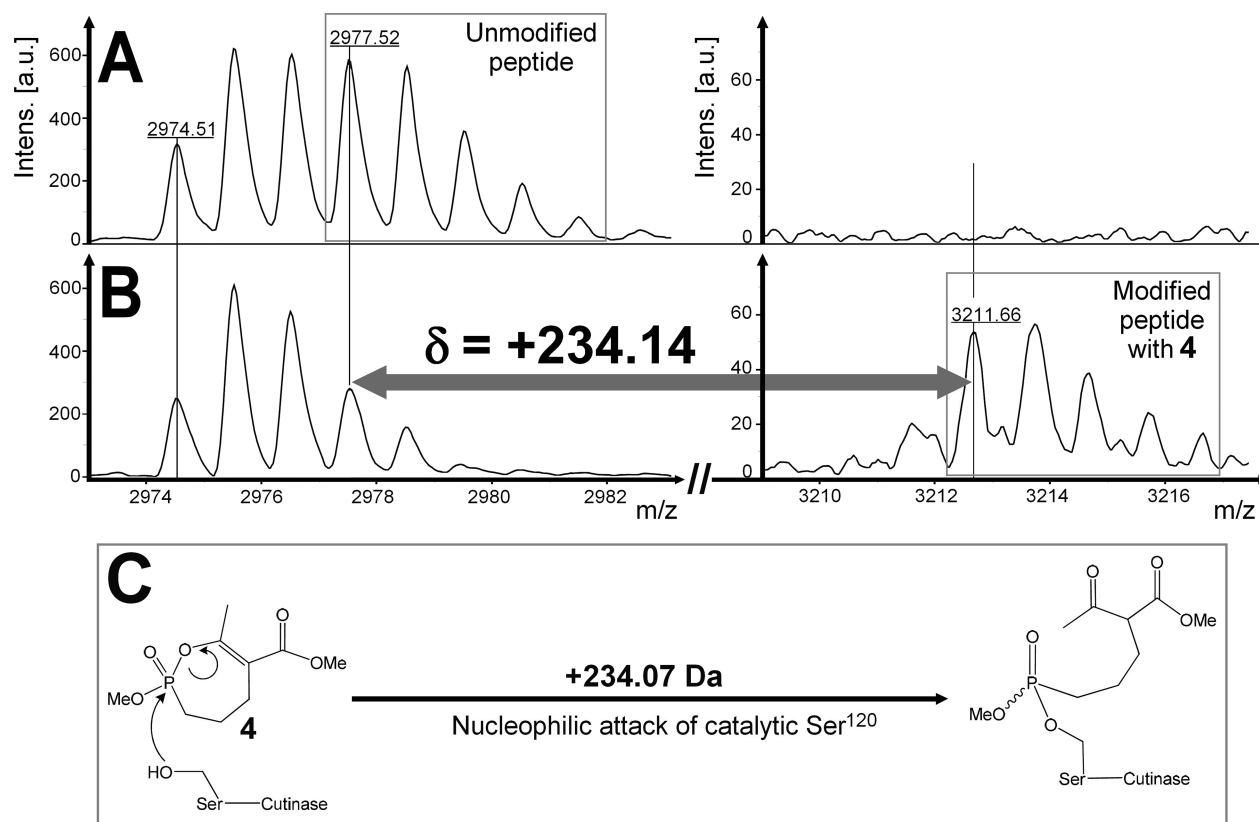


Figure 4. Peptide mass fingerprint spectra of the digested Cutinase, before (upper panels, A) and after (lower panels, B) a 30-min incubation period with compound **4** at an inhibitor molar excess $x_1 = 40$; and (C) the corresponding confirmed reaction mechanism with the active site Ser¹²⁰. (A and B) Zoom on the region of interest. (Left panels) Region of the unmodified peptide C¹⁰⁹–R¹³⁸ (C¹⁰⁹PDATLIAGGYS¹²⁰QGAALAAASIEDLDSAIR¹³⁸) containing the catalytic Ser¹²⁰ and detected at 2977.52 Da. This multiplet peak is overlaid with a first one corresponding to peptide V¹⁶⁹–R¹⁹⁶, detected at 2974.51 Da. (Right panels) Region in which a new peptide was expected to occur resulting from the covalent binding of compound **4** to the catalytic serine. Mass shifts were calculated as the difference between the experimental m/z of the modified peptide and the theoretical m/z of the unmodified catalytic peptide. The expected exact mass shift is +234.07 Da.

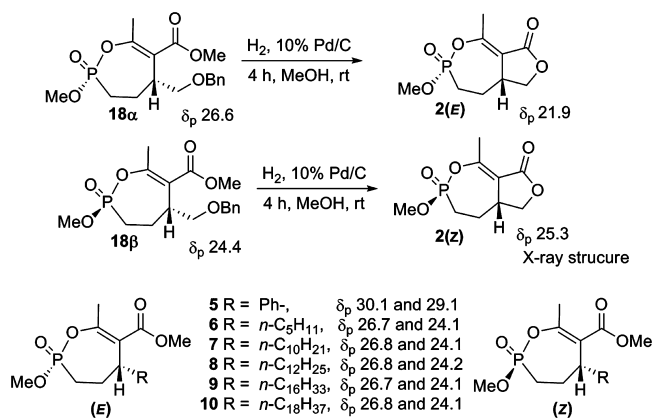
opportunity to investigate the enzyme selectivity of this class of compounds or their analogs, based on structure modification of the parent molecule. In that way, phosphonates have garnered a reputation for being excellent structural mimics of natural phosphates. It is also well-known that, for phosphonate compounds, the mode of inhibition involves the formation of a nonhydrolyzable covalent bond between the phosphorus and the catalytic O γ serine residue of the enzyme active site.¹⁹ For this purpose, novel synthetic routes were proposed and a full library of new monocyclic enol-phosphonate compounds, analogous to either Cyclophostin or Cyclipostins (Schemes 1 and 2), has been synthesized.

The strategy applied, involving palladium(0)-catalyzed addition of methyl acetoacetate to phosphono allylic carbonates and selective monodemethylation and cyclization, allowed for the custom synthesis of monocyclic phosphonates substituted at the phosphorus atom or at the C-5 position. The monocyclic phosphonates **6**–**10** were formed as mixtures of diastereoisomers which were further easily separated and purified. The fast eluting (α) isomer had a signal in the ³¹P NMR spectrum at 26.8 ppm, whereas the slower eluting (β) isomer had a signal at 24.2 ppm, consistent with all examples (**6**–**10**) studied. We had earlier demonstrated in the synthesis of the racemic bicyclic phosphonate analogs of cyclophostin **2**(α) and **2**(β)¹⁵ that the monocyclic phosphonate isomer **18** β with the upfield shift (24.2 ppm) had the phosphonate methoxy and the 5-hydrogen in a *cis* conformation (5-alkyl substituent is therefore *trans* to

the methoxy) (Scheme 3). Consequently, the isomer **18** α with the downfield shift (26.6 ppm) had the phosphonate methoxy and the 5-hydrogen substituent *trans* to each other.

From these experimental observations, combined with the obtained single crystal X-ray diffraction structure of **10**(α) (Figure 1), it was then possible to assign without any ambiguity the *trans*- α and *cis*- β relative stereochemistry of the monocyclic phosphonates **5**–**10**.

Scheme 3. Relative Stereochemistry of the Monocyclic Phosphonates **5**–**10**



Overall, the chemical pathways developed here make possible the synthesis of large libraries of fully customizable enol-phosphorus compounds with controlled *cis* or *trans* diastereochemistry.

Based on their structural properties previously depicted in Scheme 1, these organophosphorous compounds have been tested for their abilities to inhibit six lipolytic enzymes, including mammalian digestive lipases (HPL, DGL, and GPLRP2) and three microbial lipases (Cutinase, Rv0183, and LipY). In view of the specific mechanism of action of these lipolytic enzymes,²⁷ the Michaelis–Menten–Henri model no longer applies⁴⁷ and therefore the K_m , K_i and IC_{50} values often estimated for lipases are irrelevant when insoluble substrates and/or inhibitors are involved. The use of more appropriate kinetic constants such as the inhibitor molar excess leading to 50% lipase inhibition, *i.e.* x_{150} value,⁴² is thus recommended when assessing the inhibitory potency of insoluble inhibitors, such as these cyclic enol-phosphorus derivatives. Thereby, an x_{150} value of 0.5 is synonymous with a 1:1 stoichiometric ratio between the inhibitor and the lipase and is therefore the highest level of inhibitory activity that can be achieved. Regarding lipase stereopreference, this parameter has also been studied on the basis of the Diastereoselectivity Index (DI)⁴³ between the two diastereoisomers *trans*-(α) and *cis*-(β) (see eq 1 in the Experimental Section).

Regarding the three microbial lipases, Cutinase, Rv0183 and LipY were all inhibited by the cyclic enol-phosphorus compounds. The fused butyrolactone did not appear to be necessary for activity since the monocyclic diastereoisomers showed similar or even better x_{150} values than those of the bicycles **1** and **2**(α , β). However, the presence of ester functionality in conjugation with the enol-phosphate or phosphonate bond was found essential to the biological activity. This effect was well illustrated when comparing **3** with **4**. These two compounds only differ at the exocyclic functionality: the alcohol in **3** is a poor leaving group and **3** is an extremely poor inhibitor, while compound **4** with the ester group is more potent. This phenomenon, which depicts the electron-withdrawing contribution of the ester moiety in increasing the leaving group characteristics of the enol from the P-center, is in line with mass spectrometry analyses confirming that the inhibition is due to phosphorylation of the catalytic serine residue for each enzyme, as depicted in Figure 4C. Such findings demonstrate that the enol-phosphonate really acts as a leaving group on reaction with the active site serine, leading to the formation of a stoichiometric covalent enzyme–inhibitor complex. The fact that comparable results had also been observed when testing the inhibitory properties of the phosphonate analogs of Cyclophostin (*i.e.*, compounds **1** to **4**) against the housefly AChE (CSMA strain) therefore suggests a similar mode of action of this enzyme.^{15,16,21} The *trans*-**2**(α) diastereoisomer of bicyclic phosphonate analogs of Cyclophostin was also found to be almost 10 times more potent than the *cis*-**2**(β) stereoisomer when tested against human AChE.¹⁵ Based on these previous experimental kinetic data, it was suggested that the diastereopreference could be due to some specific initial contacts between the inhibitor and the active site amino acid residues, which ultimately led to a successful inhibition.¹⁶ In the present study, LipY was barely affected by the bicyclic molecules **1** and **2**(α , β), while Rv0183 did not discriminate between the two conformations (DI = 1.9%) and Cutinase exhibited a slight stereopreference (DI = 32.3%) for the *trans* isomer **2**(β). These results illustrate the difference in

selectivity exerted by the three lipases. Indeed, although the best monocyclic phosphonate inhibitors all displayed a *cis* conformation (*i.e.* (β) isomers), the group on the γ -carbon of the phosphonate ring significantly affects and modifies the biological activity of the monocyclic analogs. Such structural changes lead to more selective inhibitors toward the microbial lipases tested. Rv0183 indeed reacts selectively with Cyclophostin analogs bearing medium to long alkyl chains, while LipY is only fully inactivated by highly lipophilic compounds. Cutinase, however, is found to be less selective since it reacts with most of the organophosphorous compounds without any real chemopreference (Table 2). Such a high and stringent chemoselectivity exerted by Rv0183 and LipY, or conversely the lower one in the case of Cutinase, is consistent with the respective substrate specificity of these three lipolytic enzymes.^{32–34,36,37}

Comparisons with the potent but nonselective lipase inhibitor Orlistat were very instructive. Indeed, the inhibitory power exerted by compounds **11**, **12**, and **7**(β) on Cutinase, LipY, and Rv0183, respectively, was 4.5 to 176 times higher than that of Orlistat acting on the same lipases. Moreover, with x_{150} values as low as 0.56 for **11** acting on Cutinase, which is close to the lowest achievable value (the theoretical minimum value being 0.50), these phosphorus compounds react in a quasi-stoichiometric way with these enzymes. By contrast, the enol-phosphonates had no effects on HPL, DGL, and GPLRP2, while these mammalian lipases were strongly inhibited by Orlistat. *In silico* molecular docking experiments with **7**(β) suggest that these seven-membered ring phosphorus molecules can enter the active site of HPL, DGL, and GPLRP2 but cannot interact with the catalytic serine residue. In each case, the lipophilic alkyl chains of the best scoring positions of **7**(β) would be stabilized by hydrophobic residues located near the active site (Figure 3, white color). In this binding mode, however, the reactive oxaphosphepine ring of **7**(β) would adopt a nonproductive orientation: the phosphorus atom is indeed found in the opposite position making it impossible to react with the catalytic serine.

Taken together, all these findings suggest that this series of enol-phosphonates **6–12** may be selective inhibitors of these families of microbial lipolytic enzymes, *i.e.*, Cutinase, monoglyceride lipase, and hormone sensitive lipase families.

It has been shown recently that the use of Orlistat could significantly reduce the growth of *Mycobacterium smegmatis*,¹⁰ a nonpathogen *Mycobacterium* species, and of *Mycobacterium bovis* BCG⁹ which is closely related to the pathogen *Mycobacterium tuberculosis*. In addition, some recent papers pointed out the fact that Orlistat could also target potentially essential enzymes involved either in the mycobacteria cell wall biosynthesis such as the Cutinase-like Rv3802c¹¹ or in the hydrolysis of stored triacylglycerols during persistence and reactivation phases such as LipY.³⁶ Fighting tuberculosis is still challenging, not only in third world countries but also in the so-called industrialized world, due to the impressive recrudescence of this major infectious disease. In that context, our encouraging results on the selective inhibition of Cutinase as well as of pure microbial lipolytic enzymes from *Mycobacterium tuberculosis* suggest that this new class of phosphonate analogs of Cyclophostin and Cyclophostins could be potential scaffolds and may provide useful leads for the further development of more selective antimicrobial agents, including antimycobacterial compounds. In particular, thanks to our synthetic routes, we have clearly showed that modulation of the lipophilicity and/or

functionalization at the C-5 carbon atom or at the phosphorus can be exploited to either attenuate or increase the affinity of one inhibitor to target a specific microbial lipase.

CONCLUSION

This work provided the first fundamental premise for the understanding of the structure–activity relationships of monocyclic enol-phosphonate analogs in connection with the inhibition of several lipases having distinct substrate specificities. Moreover, the major interest in this new family of phosphonate inhibitors is that their chemical structure is flexible at will. The strategy developed here, involving palladium(0)-catalyzed addition of methyl acetoacetate to phosphono allylic carbonates followed by selective monodemethylation and cyclization, allows for the synthesis of a large variety of fully customizable monocyclic enol-phosphonates substituted at the C-5 position. Furthermore, the methyl phosphonate ester can be easily *trans*-esterified to give long chain ester compounds analogous to Cycloipostins. This flexibility makes it possible to design selective inhibitors for a given enzyme. In order to shed more light on the influence of the chirality at both phosphorus and carbon centers on lipase inhibition, further experiments are currently underway and will be reported in due course.

EXPERIMENTAL SECTION

Chemistry—Synthesis of Compounds 1 to 12. *General Experimental.* All reactions were carried out in oven-dried glassware under an atmosphere of argon unless otherwise noted. ^1H , ^{13}C , and ^{31}P NMR spectra were recorded at 300, 75, and 121 MHz respectively. ^1H NMR spectra are referenced to CDCl_3 (7.27 ppm), ^{13}C NMR spectra are referenced to the center line of CDCl_3 (77.23 ppm) and ^{31}P NMR spectra are referenced to external H_3PO_4 . Coupling constants, J , are reported in Hz. Analytical thin-layer chromatography (TLC) analyses were performed on silica gel plates 60PF₂₅₄. Visualization was accomplished with UV light, KMnO_4 solution, or iodine. The syntheses of racemic **1**,²¹ racemic **2**(α) and **2**(β),¹⁵ **3**, and **4**¹⁶ as well as carbonates **13a**, **13b**, and **13c**³⁸ have already been reported. Target compounds were purified by chromatography and have purities of $\geq 95\%$ as determined by HPLC analysis conducted on an Agilent 1100 system, using a Zorbax Eclipse XBD-C18 column. Elution was performed at a flow rate of $2\text{ mL}\cdot\text{min}^{-1}$ using a gradient of $\text{H}_2\text{O}/\text{TFA}/\text{CH}_3\text{CN}$ 95:0.1:5 to $\text{H}_2\text{O}/\text{TFA}/\text{CH}_3\text{CN}$ 5:0.1:95 over 6 min or using a gradient of $\text{H}_2\text{O}/\text{TFA}/\text{CH}_3\text{CN}$ 95:0.1:5 to 100% CH_3CN over 5 min followed by a hold at 100% CH_3CN for 3 min. The compounds were detected using a diode array and ELS. The HPLC data were supported by careful analysis of the ^1H , ^{13}C , and particularly the ^{31}P NMR spectra.

*General Procedure for Synthesis of the Carbonates 13 via Cross Metathesis Reaction.*³⁹ To a solution of carbonate **13a** (1.0 mmol) and alkene (5.0–10.0 mmol) in CH_2Cl_2 (2 mL) was added Grubbs' second generation catalyst (5 mol %) followed by CuI (7 mol %). After stirring the solution for 2 min at room temperature, the septum was replaced by a condenser connected to an argon bubbler and the reaction flask was placed in an oil bath preheated to $45\text{ }^\circ\text{C}$. After completion of the reaction (TLC and ^{31}P NMR analysis), the solvent was removed under reduced pressure to give the crude product. Purification of the crude product by column chromatography (SiO_2 , 20–50% EtOAc in hexanes) gave the carbonate **13** ($E:Z \geq 10:1$).

(\pm)-(E)-1-(Dimethoxyphosphoryl)tridec-2-en-1-yl Methyl Carbonate (13d). To a solution of carbonate **13a** (1.12 g, 5.00 mmol) and 1-dodecene (11.1 mL, 50.0 mmol) in dry CH_2Cl_2 (10 mL) was added Grubbs' second generation catalyst (0.21 g, 0.25 mmol) followed by CuI (0.07 g, 0.35 mmol) to give **13d** (1.43 g, 79%). IR (neat, NaCl) 1756 cm^{-1} ; ^1H NMR (CDCl_3) δ 5.97 (1H, ddt, $J_{\text{HH}} = 15.2, 6.7\text{ Hz}$, $J_{\text{HP}} = 3.7\text{ Hz}$), 5.55 (1H, ddd, $J_{\text{HH}} = 15.2, 7.6\text{ Hz}$, $J_{\text{HP}} = 5.2\text{ Hz}$), 5.45 (1H, dd, $J_{\text{HH}} = 8.0\text{ Hz}$, $J_{\text{HP}} = 12.4\text{ Hz}$), 3.81 (d, 3H, $J_{\text{HP}} = 10.6\text{ Hz}$), 3.81

(3H, s), 3.8 (d, 3H, $J_{\text{HP}} = 10.6\text{ Hz}$), 2.08 (2H, ddd, $J_{\text{HH}} = 13.9, 6.6\text{ Hz}$, $J_{\text{HP}} = 3.4\text{ Hz}$), 1.37 (2H, t, $J_{\text{HH}} = 6.7\text{ Hz}$), 1.25 (16H, br s), 0.87 (3H, t, $J_{\text{HH}} = 6.6\text{ Hz}$); ^{13}C NMR (CDCl_3) δ 155.0 (d, $J_{\text{CP}} = 9.9\text{ Hz}$), 139.4 (d, $J_{\text{CP}} = 12.5\text{ Hz}$), 120.3 (d, $J_{\text{CP}} = 3.8\text{ Hz}$), 73.3 (d, $J_{\text{CP}} = 170.2\text{ Hz}$), 55.5, 54.0 (d, $J_{\text{CP}} = 7.2\text{ Hz}$), 32.6, 32.1, 29.8, 29.6, 29.5, 29.3, 28.8 (d, $J_{\text{CP}} = 2.4\text{ Hz}$), 22.9, 14.3; ^{31}P NMR (CDCl_3) δ 20.8, 20.5 ($E:Z = 10:1$); HRMS (FAB, NBA, MH^+) calcd for $\text{C}_{17}\text{H}_{34}\text{O}_6\text{P}$: 365.2092, found 365.2103.

(\pm)-(E)-1-(Dimethoxyphosphoryl)pentadec-2-en-1-yl Methyl Carbonate (13e). To a solution of carbonate **13a** (1.12 g, 5.00 mmol) and 1-tetradecene (12.7 mL, 50.0 mmol) in dry CH_2Cl_2 (10 mL) was added Grubbs' second generation catalyst (0.21 g, 0.25 mmol) followed by CuI (0.07 g, 0.35 mmol) to give **13e** (1.5 g, 76%). IR (neat, NaCl) 1755 cm^{-1} ; ^1H NMR (CDCl_3) δ 5.95 (1H, ddt, $J_{\text{HH}} = 15.2, 6.7\text{ Hz}$, $J_{\text{HP}} = 3.8\text{ Hz}$), 5.55 (1H, ddd, $J_{\text{HH}} = 15.2, 7.6\text{ Hz}$, $J_{\text{HP}} = 5.2\text{ Hz}$), 5.45 (1H, dd, $J_{\text{HH}} = 7.8\text{ Hz}$, $J_{\text{HP}} = 12.4\text{ Hz}$), 3.81 (d, 3H, $J_{\text{HP}} = 10.6\text{ Hz}$), 3.81 (3H, s), 3.80 (d, 3H, $J_{\text{HP}} = 10.6\text{ Hz}$), 2.08 (2H, ddd, $J_{\text{HH}} = 13.9, 6.7\text{ Hz}$, $J_{\text{HP}} = 3.5\text{ Hz}$), 1.37 (2H, t, $J_{\text{HH}} = 6.7$), 1.24 (18H, br s), 0.87 (3H, t, $J_{\text{HH}} = 6.6\text{ Hz}$); ^{13}C NMR (CDCl_3) δ 154.9 (d, $J_{\text{CP}} = 9.8\text{ Hz}$), 139.3 (d, $J_{\text{CP}} = 12.5\text{ Hz}$), 120.3 (d, $J_{\text{CP}} = 3.8\text{ Hz}$), 73.2 (d, $J_{\text{CP}} = 170.3\text{ Hz}$), 55.5, 54.0 (d, $J_{\text{CP}} = 7.2\text{ Hz}$), 32.6, 32.1, 29.9, 29.8, 29.7, 29.6, 29.5, 29.4, 29.3, 28.8 (d, $J_{\text{CP}} = 2.4\text{ Hz}$), 22.9, 14.3; ^{31}P NMR (CDCl_3) δ 20.9, 20.5 ($E:Z = 8:1$); HRMS (FAB, NBA, MH^+) calcd for $\text{C}_{19}\text{H}_{37}\text{O}_6\text{PNa}$: 415.2225, found 415.2227.

(\pm)-(E)-1-(Dimethoxyphosphoryl)nonadec-2-en-1-yl Methyl Carbonate (13f). To a solution of carbonate **13a** (1.12 g, 5.00 mmol) and 1-octadecene (8.0 mL, 25 mmol) in dry CH_2Cl_2 (10 mL) was added Grubbs' second generation catalyst (0.21 g, 0.25 mmol) followed by CuI (0.07 g, 0.35 mmol) to give **13f** (1.57 g, 70%). IR (neat, NaCl), 1755 cm^{-1} ; ^1H NMR (CDCl_3) δ 5.96 (1H, ddt, $J_{\text{HH}} = 14.6, 7.1\text{ Hz}$, $J_{\text{HP}} = 3.8\text{ Hz}$), 5.55 (1H, ddd, $J_{\text{HH}} = 7.7, 15.2\text{ Hz}$, $J_{\text{HP}} = 5.2\text{ Hz}$), 5.44 (1H, dd, $J_{\text{HH}} = 7.8\text{ Hz}$, $J_{\text{HP}} = 12.3\text{ Hz}$), 3.82 (3H, s), 3.81 (d, 3H, $J_{\text{HP}} = 10.6\text{ Hz}$), 3.81 (d, 3H, $J_{\text{HP}} = 10.6\text{ Hz}$), 2.1 (2H, ddd, $J_{\text{HH}} = 7, 13.7\text{ Hz}$, $J_{\text{HP}} = 3.2\text{ Hz}$), 1.37 (2H, t, $J_{\text{HH}} = 6.5\text{ Hz}$), 1.25 (26H, br s), 0.87 (3H, t, $J_{\text{HH}} = 6.44\text{ Hz}$); ^{13}C NMR (CDCl_3) δ 155 (d, $J_{\text{CP}} = 9.8\text{ Hz}$), 139.3 (d, $J_{\text{CP}} = 12.4\text{ Hz}$), 120.3 (d, $J_{\text{CP}} = 3.8\text{ Hz}$), 73.3 (d, $J_{\text{CP}} = 170.3\text{ Hz}$), 55.5, 54.0 (d, $J_{\text{CP}} = 7.3\text{ Hz}$), 32.6, 32.1, 29.9, 29.8, 29.7, 29.6, 29.5, 29.3, 28.8, 28.7, 22.9, 14.4; ^{31}P NMR (CDCl_3) δ 20.8, 20.5 ($E:Z = 10:1$); HRMS (FAB, NBA, MNa^+) calcd for $\text{C}_{23}\text{H}_{45}\text{O}_6\text{PNa}$: 471.2851, found 471.2860.

(\pm)-(E)-1-(Dimethoxyphosphoryl)henicos-2-en-1-yl Methyl Carbonate (13g). To a solution of carbonate **13a** (0.67 g, 3 mmol) and 1-eicocene (4.21 mL, 15 mmol) in dry CH_2Cl_2 (6 mL) was added Grubbs' second generation catalyst (0.13 g, 0.15 mmol) followed by CuI (0.04 g, 0.21 mmol) to give **13g** (1.1 g, 70%). IR (neat, NaCl) 1755 cm^{-1} ; ^1H NMR (CDCl_3) δ 5.97 (1H, ddt, $J_{\text{HH}} = 14.9, 6.7\text{ Hz}$, $J_{\text{HP}} = 3.8\text{ Hz}$), 5.56 (1H, ddd, $J_{\text{HH}} = 15.1, 7.7\text{ Hz}$, $J_{\text{HP}} = 5.3\text{ Hz}$), 5.46 (1H, dd, $J_{\text{HH}} = 7.8\text{ Hz}$, $J_{\text{HP}} = 12.2\text{ Hz}$), 3.82 (3H, s), 3.81 (d, 3H, $J_{\text{HP}} = 10.6\text{ Hz}$), 3.81 (d, 3H, $J_{\text{HP}} = 10.6\text{ Hz}$), 2.1 (2H, $J_{\text{HH}} = 6.7, 13.7\text{ Hz}$, $J_{\text{HP}} = 3.4\text{ Hz}$), 1.39 (2H, t, $J_{\text{HH}} = 6.7\text{ Hz}$), 1.26 (30 H, br s), 0.88 (3H, t, $J_{\text{HH}} = 6.7\text{ Hz}$); ^{13}C NMR (CDCl_3) δ 155.0 (d, $J_{\text{CP}} = 9.8\text{ Hz}$), 139.4 (d, $J_{\text{CP}} = 12.5\text{ Hz}$), 120.3 (d, $J_{\text{CP}} = 3.8\text{ Hz}$), 73.3 (d, $J_{\text{CP}} = 170.3\text{ Hz}$), 55.5, 54.0 (d, $J_{\text{CP}} = 7.1\text{ Hz}$), 32.6, 32.1, 30, 29.9, 29.8, 29.6, 29.5, 29.3, 28.8 (d, $J_{\text{CP}} = 2.4\text{ Hz}$), 22.9, 14.4; ^{31}P NMR (CDCl_3) δ 20.8, 20.5 ($E:Z = 10:1$); HRMS (FAB, NBA, MH^+) calcd for $\text{C}_{25}\text{H}_{49}\text{O}_6\text{PNa}$: 499.3164, found 499.3170.

General Procedure for Synthesis of Vinyl Phosphonates 14. To a stirring solution of carbonate **13** (1 mmol) and methyl acetoacetate (3 mmol) in dry THF (2.5 mL) was added $\text{Pd}_2(\text{dba})_3$ (0.02 mmol) followed by dppe (0.5 mmol), and the resulting mixture was stirred at room temperature for 3–4 min. The septum was replaced by a condenser connected to an argon bubbler, and the reaction flask was placed in an oil bath preheated to $45\text{ }^\circ\text{C}$. After completion of the reaction (TLC and ^{31}P NMR analysis), the reaction mixture was partitioned between brine and EtOAc . The organic layer was collected, and the aqueous layer was extracted with additional EtOAc . The combined organic layers were dried over anhydrous Na_2SO_4 and evaporated under reduced pressure to give the crude product. Purification of the crude by column chromatography (SiO_2 , 20–70% EtOAc in hexanes) gave the vinyl phosphonate **14**.

(±)-(*E*)-Methyl 2-Acetyl-5-(dimethoxyphosphoryl)-3-phenylpent-4-enoate (**14b**) and (2*Z*,3*Z*)-Methyl 5-(Dimethoxyphosphoryl)-2-(1-hydroxyethylidene)-3-phenylpent-3-enoate (**15**). To a solution of carbonate **13b** (0.75 g, 2.5 mmol) and methyl acetoacetate (0.87 mL, 7.6 mmol) in THF (6 mL) were added Pd₂(dba)₃ (0.05 g, 0.05 mmol) and dppe (0.05 g, 0.13 mmol) to give **14b** as a 1:1 diastereoisomeric mixture (0.32 g, 46%). Pale yellow solid; IR (neat), 1742, 1714 cm⁻¹; ¹H NMR (CDCl₃) δ 7.26 (m, 5H), 6.73 (1H, m), 5.75 (1H, m), 4.28 (1H, m), 4.1 (1H, d, *J*_{HH} = 11.27 Hz), 3.66 (6H, m), 3.61 (3H, s), 2.14 (3H, s); ¹³C NMR (CDCl₃) δ 200.4 (200.3), 167.7 (167.3), 152.3 (152.26) (d, *J*_{CC} = 5.2 Hz), 137.9 (137.6), 129.1 (128.9), 128.2 (128.1), 128.1, 127.8 (127.6), 117.8 (117.5) (d, *J*_{CP} = 185.4 Hz), 64.1 (63.5), 52.7 (52.5), 52.3 (d, *J*_{CP} = 5.7 Hz), 49.3 (48.9) (d, *J*_{CP} = 22.2 Hz), 30.4 (30.1); ³¹P NMR (CDCl₃) δ 20.87, 20.1 ppm; HRMS (FAB, NBA, MH⁺) calcd for C₁₆H₂₁O₆P: 340.1153, found 341.1157 and **15** (0.34 g, 47%). White solid; IR (neat) 1646, 1611 cm⁻¹; ¹H NMR (CDCl₃) δ 13.02, (1H, s), 7.37–7.25 (5H, m), 6.18 (1H, *J*_{HH} = 7.6 Hz), 3.76 (6H, d, *J* = 10.87 Hz), 3.71 (3H, s), 2.7 (2H, dd, *J*_{HH} = 7.6 Hz, *J*_{HP} = 22.6 Hz), 1.88 (3H, s); ¹³C NMR (CDCl₃) δ 175.5, 172.9, 140.7, 138.2, 128.9, 128.0, 126.3, 121.1, 99.4, 53.0 (d, *J*_{CP} = 11.43 Hz), 52.2, 27.9 (d, *J*_{CP} = 139.88 Hz), 19.8; ³¹P NMR (CDCl₃) δ 30.46; HRMS (FAB, NBA, MH⁺) calcd for C₁₆H₂₂O₆P: 340.1153, found 341.1150.

(±)-(*E*)-Methyl 2-Acetyl-3-(2-(dimethoxyphosphoryl)vinyl)octanoate (**14c**). To a solution of carbonate **14c** (0.29 g, 1.0 mmol) and methyl acetoacetate (0.33 mL, 3.0 mmol) in dry THF (2 mL) were added Pd₂(dba)₃ (0.02 g, 0.02 mmol) and dppe (0.02 g, 0.05 mmol) to give **14c** as a 1:1 mixture of diastereoisomers (1.17 g, 70%). Pale yellow oil; IR (neat, NaCl) 1743, 1717; ¹H NMR (CDCl₃) δ 6.55 (0.5H, ddd, *J*_{HH} = 17.13, 9.5 Hz, *J*_{HP} = 21.5 Hz), 6.45 (0.5H, ddd, *J*_{HH} = 17.13, 9.5 Hz, *J*_{HP} = 21.5 Hz), 5.68 (0.5H, dd, *J*_{HH} = 17.13 Hz, *J*_{HP} = 21.5 Hz), 5.61 (0.5H, ddd, *J*_{HH} = 17.13 Hz, *J*_{HP} = 21.5 Hz), 3.67 (9H, m), 3.51 (1H, 2d, *J*_{HH} = 9.4, 9.3 Hz), 2.95 (1H, 2q, *J*_{HH} = 9.4 and 9.4 Hz), 2.21 (1.5H, s), 2.15 (1.5H, s), 1.28 (8H, m); 0.83 (3H, t, *J*_{HH} = 6.44 Hz); ¹³C NMR (CDCl₃) δ 201.3, 168.6 (168.4), 153.4 (153.3) (d, *J*_{CP} = 4.6 Hz), 118.8 (118.7) (d, *J*_{CP} = 184.5 Hz), 63.8 (63.7) (d, *J*_{CP} = 1.0 Hz), 52.7 (52.5), 52.4 (d, *J*_{CP} = 5.6 Hz), 44.0 (43.9) (d, *J*_{CP} = 21.8 Hz), 31.8 (31.6), 31.5 (d, *J*_{CP} = 1.3 Hz), 30.1 (29.9), 26.8 (26.7), 22.5, 14.0; ³¹P NMR (CDCl₃) δ 20.7, 20.6; HRMS (FAB, NBA, MH⁺) calcd for C₁₅H₂₇O₆PNa: 357.1442, found 357.1450.

(±)-(*E*)-Methyl 2-Acetyl-3-(2-(dimethoxyphosphoryl)vinyl)tridecanoate (**14d**). To the stirring solution of carbonate **13d** (0.182 g, 0.50 mmol) and methyl acetoacetate (0.17 mL, 1.5 mmol) in dry THF (1 mL) was added Pd₂(dba)₃ (0.01 g, 0.01 mmol) followed by dppe (0.10 g, 0.025 mmol) to give **14d** as a 1:1 mixture of diastereoisomers (0.16 g, 78%). Pale yellow oil; IR (neat, NaCl) 1743, 1719 cm⁻¹; ¹H NMR (CDCl₃) δ 6.59 (0.5H, ddd, *J*_{HH} = 17.1, 9.6 Hz, *J*_{HP} = 21.5 Hz), 6.49 (0.5H, ddd, *J*_{HH} = 17.1, 9.6 Hz, *J*_{HP} = 21.5 Hz), 5.7 (0.5H, dd, *J*_{HH} = 17.1 Hz, *J*_{HP} = 21.5 Hz), 5.65 (0.5H, dd, *J*_{HH} = 17.1 Hz, *J*_{HP} = 21.5 Hz), 3.67 (9H, m), 3.54 (1H, 2d, *J*_{HH} = 9.4 and 9.2 Hz), 2.98 (1H, 2q, *J*_{HH} = 9.3 Hz), 2.24 (1.6H, s), 2.18 (1.4H, s), 1.23 (30H, br s), 0.87 (3H, t, *J*_{HH} = 6.7 Hz); ¹³C NMR (CDCl₃) δ 201.5, 168.7 (168.5), 153.5 (d, *J*_{CP} = 9.1 Hz), 118.8 (d, *J*_{CP} = 171.7 Hz), 63.9 (63.8), 52.8 (52.7), 52.5 (d, *J*_{CP} = 5.4 Hz), 44.3 (44), 32.1, 31.9 (31.8), 30.3 (30.1), 29.8, 29.6, 29.5, 27.3 (27.20), 22.9, 14.3; ³¹P NMR (CDCl₃) δ 20.7, 20.6; HRMS (FAB, NBA, MH⁺) calcd for C₂₀H₃₈O₆P: 405.2406, found 405.2403.

(±)-(*E*)-Methyl 2-Acetyl-3-(2-(dimethoxyphosphoryl)vinyl)pentadecanoate (**14e**). To a stirring solution of carbonate **13e** (1.26 g, 3.20 mmol) and methyl acetoacetate (1.05 mL, 9.60 mmol) in dry THF (6.5 mL) was added Pd₂(dba)₃ (0.06 g, 0.64 mmol) followed by dppe (0.06 g, 0.16 mmol) to give **14e** as a 1:1 mixture of diastereoisomers (1.13 g, 80%). Pale yellow oil; IR (neat, NaCl) 1743, 1719 cm⁻¹; ¹H NMR (CDCl₃) δ 6.59 (0.5H, ddd, *J*_{HH} = 17.1, 9.5 Hz, *J*_{HP} = 21.5 Hz), 6.49 (0.5H, ddd, *J*_{HH} = 17.1, 9.5 Hz, *J*_{HP} = 21.5 Hz), 5.72 (0.5H, dd, *J*_{HH} = 17.1 Hz, *J*_{HP} = 21.5 Hz), 5.65 (0.5H, dd, *J*_{HH} = 17.1 Hz, *J*_{HP} = 21.5 Hz), 3.71 (9H, m), 3.5 (1H, 2d, *J*_{HH} = 9.4 and 9.2 Hz), 2.98 (1H, 2q, *J*_{HH} = 9.1 and 9.3 Hz, *J*_{HH} = 1.6 Hz), 2.21 (1.5H, s), 2.15 (1.5H, s), 1.22 (22H, br s), 0.88 (3H, t, *J*_{HH} = 6.7 Hz); ¹³C NMR

(CDCl₃) δ 201.5, 168.7 (168.6), 153.5 (d, *J*_{CP} = 4.4 Hz), 118.9 (185) (d, *J*_{CP} = 184.8 Hz), 63.9 (63.8), 52.6 (52.7), 52.5 (d, *J*_{CP} = 5.6 Hz), 44.3 (44), 32.1, 31.9 (31.8), 30.3 (30.1), 29.9, 29.8, 29.7, 29.6, 29.5, 27.3 (27.2), 22.9, 14.3; ³¹P NMR (CDCl₃) δ 20.7, 20.6; HRMS (FAB, MH⁺) calcd for C₂₂H₄₂O₆P: 433.2718, found 433.2720.

(±)-(*E*)-Methyl 2-Acetyl-3-(2-(dimethoxyphosphoryl)vinyl)nonadecanoate (**14f**). To a stirring solution of carbonate **13f** (0.45 g, 1.0 mmol) and methyl acetoacetate (0.64 mL, 3.0 mmol) in dry THF (2 mL) was added Pd₂(dba)₃ (0.02g, 0.02 mmol) followed by dppe (0.02g, 0.05 mmol) to give **14f** as a 1:1 mixture of diastereoisomers (0.36 g, 72%). Waxy solid; IR (neat, NaCl) 1743, 1637 cm⁻¹; ¹H NMR (CDCl₃) δ 6.59 (0.5H, ddd, *J*_{HH} = 17.1, 9.5 Hz, *J*_{HP} = 21.5 Hz), 6.45 (0.5H, ddd, *J*_{HH} = 17.1, 9.4 Hz, *J*_{HP} = 21.5 Hz), 5.72 (0.5H, dd, *J*_{HH} = 17.1 Hz, *J*_{HP} = 21.5 Hz), 5.65 (0.5H, dd, *J*_{HH} = 17.1 Hz, *J*_{HP} = 21.5 Hz), 3.71 (9H, m), 3.54 (1H, 2d, *J*_{HH} = 9.4 and 9.2 Hz), 2.97 (1H, 2q, *J*_{HH} = 9.1 and 9.3 Hz), 2.21 (1.5H, s), 2.15 (1.5H, s), 1.22 (30H, br s), 0.85 (3H, t, *J*_{HH} = 6.66 Hz); ¹³C NMR (CDCl₃) δ 201.3, 168.6 (168.5), 153.4 (153.3) (d, *J*_{CP} = 8.4 Hz), 118.8 (118.6) (d, *J*_{CP} = 184.3 Hz), 63.8 (63.7), 52.7 (52.5), 52.7 (d, *J*_{CP} = 5.6 Hz), 44.2 (43.9) (d, *J*_{CP} = 2.2 Hz), 32.1, 31.8 (31.7), 30.2 (30), 29.9, 29.8, 29.7, 29.6, 29.5, 29.4, 27.2 (27.1), 22.8, 14.3; ³¹P NMR (CDCl₃) δ 20.7, 20.6; HRMS (FAB, NBA, MH⁺) calcd. for C₂₆H₅₀O₆P: 485.3345, found 489.3340.

(±)-(*E*)-Methyl 2-Acetyl-3-(2-(dimethoxyphosphoryl)vinyl)heneicosanoate (**14g**). To a stirring solution of carbonate **13g** (0.48 g, 1.0 mmol) and methyl acetoacetate (0.33 mL, 3.0 mmol) in dry THF (2 mL) was added Pd₂(dba)₃ (0.02 g, 0.02 mmol) followed by dppe (0.02 g, 0.05 mmol) to give **14g** as a 1:1 mixture of diastereoisomers (0.35 g, 70%). Pale yellow oil; IR (neat, NaCl) 1742, 1713 cm⁻¹; ¹H NMR (CDCl₃) δ 6.56 (0.5H, ddd, *J*_{HH} = 17.1, 9.5 Hz, *J*_{HP} = 21.4 Hz), 6.45 (0.5H, ddd, *J*_{HH} = 17.1, 9.5 Hz, *J*_{HP} = 21.5 Hz), 5.67 (0.5H, dd, *J*_{HH} = 17.1 Hz, *J*_{HP} = 21.5 Hz), 5.60 (0.5H, dd, *J*_{HH} = 17.1 Hz, *J*_{HP} = 21.5 Hz), 3.67 (9H, m), 3.54 (1H, 2d, *J*_{HH} = 9.4 and 9.2 Hz), 2.97 (1H, 2q, *J*_{HH} = 9.4 and 9.2 Hz), 2.21 (1.5H, s), 2.15 (1.5H, s), 1.21 (34H, br s), 0.84 (3H, t, *J*_{HH} = 6.6 Hz); ¹³C NMR (CDCl₃) δ 201.3, 168.6 (168.4), 153.4 (153.3) (d, *J*_{CP} = 4.6 Hz), 118.8 (118.6) (d, *J*_{CP} = 184.6 Hz), 63.8 (63.7), 52.7 (52.5), 52.4 (d, *J*_{CP} = 5.5 Hz), 44.2 (43.9) (d, *J*_{CP} = 2.3 Hz), 32.0, 31.8 (31.7), 30.2 (30), 29.9, 29.8, 29.7, 29.6, 29.5, 29.4, 27.2 (27.1), 22.8, 14.3; ³¹P NMR (CDCl₃) δ 20.7, 20.6; HRMS (FAB, NBA, MH⁺) calcd for C₂₆H₅₀O₆P: 485.3345, found 489.3340.

General Procedure for Hydrogenation of Vinyl Phosphonate. To a solution of vinyl phosphonate **14** (1 mmol) in methanol (3 mL) was added 10% palladium on charcoal (0.07 g). The solution was first flushed with argon and then with hydrogen gas. A reservoir of hydrogen was provided by a balloon. After completion of the reaction (³¹P NMR analysis), the reaction mixture was filtered through Celite which was washed with additional CH₂Cl₂. The solvent was evaporated under reduced pressure to give the saturated phosphonate **16**.

(±)-Methyl 2-Acetyl-5-(dimethoxyphosphoryl)-3-phenylpentanoate (**16b**). To a solution of **14b** (or **15**) (0.29 g, 0.84 mmol) in methanol (3 mL) were added palladium on charcoal (0.09 g) and hydrogen gas to give the saturated phosphonate **14b** as a 1:1 mixture of diastereoisomers (0.30 g, 100%). Colorless oil; IR (neat, NaCl) 1745, 1717 cm⁻¹; ¹H NMR (CDCl₃) δ 7.34 (m, 5H), 4.28 (1H, m), 4.1 (1H, d, *J*_{HH} = 11.27 Hz), 3.66 (6H, m), 3.61 (3H, s), 2.14 (3H, s); ¹³C NMR (CDCl₃) δ 201.8, 168.8 (168.2), 139.5 (139.2), 129.1, 128.8, 128.4, 127.7, 127.6, 66.6 (65.8), 52.8, 52.5 (d, *J*_{CP} = 6.5 Hz), 46.1 (45.6) (d, *J*_{CP} = 19.1 Hz), 30.3 (30.0), 26.9 (26.8) (d, *J*_{CP} = 16.4 Hz), 23.5 (23.4), 21.6 (d, *J*_{CP} = 8.7 Hz); ³¹P NMR (CDCl₃) δ 34.6 ppm; HRMS (FAB, MH⁺) calcd for C₁₆H₂₄O₆P: 343.1310, found 343.1311.

(±)-Methyl 2-Acetyl-3-(2-(dimethoxyphosphoryl)ethyl)octanoate (**16c**). To a solution of **14c** (0.650 g, 1.96 mmol) in methanol (5 mL) were added palladium on charcoal (0.21 g) and hydrogen gas to give the saturated phosphonate **16c** as a 1:1 mixture of diastereoisomers (0.65 g, 100%). Colorless oil; IR (neat, NaCl) 1739, 1716 cm⁻¹; ¹H NMR (CDCl₃) δ 3.73 (9H, m), 3.45 (1H, d, *J*_{HH} = 8.3 Hz), 2.26 (1H, br s), 2.23 (4H, s), 1.67 (m, 4H), 1.25 (br, 8H), 0.87 (t, 3H, *J*_{HH} = 6.7

Hz); ^{13}C NMR (CDCl_3) δ 202.9, 169.7 (169.69), 63.2(63.1), 52.6, 52.5 (d, $J_{\text{CP}} = 6.5$ Hz), 38.1 (d, $J_{\text{CP}} = 17.2\text{a}$ Hz), 32.0 (d, $J_{\text{CP}} = 7.1$ Hz), 30.6 (30.4), 29.6, 26.1, 22.7, 14.2; ^{31}P NMR (CDCl_3) δ 35.0, 34.9; HRMS (FAB, NBA, MH^+) calcd for $\text{C}_{15}\text{H}_{29}\text{O}_6\text{P}$: 336.1780, found 337.1779.

(\pm)-Methyl 2-Acetyl-3-(2-(dimethoxyphosphoryl)ethyl)tridecanoate (**16d**). To the solution of **14d** (0.44 g, 1.08 mmol) in methanol (5 mL) were added palladium on charcoal (0.01 g) and hydrogen gas to give the saturated phosphonate **16d** as a 1:1 mixture of diastereoisomers (0.44 g, 100%). Colorless oil; IR (neat, NaCl) 1737, 1712 cm^{-1} ; ^1H NMR (CDCl_3) δ 3.73 (6H, d, $J_{\text{HD}} = 10.8$ Hz), 3.73 (3H, app d), 3.45 (1H, d, $J_{\text{HH}} = 8.3$ Hz), 2.26 (1H, br s), 2.23 (3H, s), 1.76–1.6 (4H, m), 1.25 (18 H, br s), 0.88 (3H, t, $J_{\text{HH}} = 6.44$ Hz); ^{13}C NMR (CDCl_3) δ 202.9, 169.7, 63.2, 52.6, 52.5, 38.2 (38), 32.1, 30.5 (d, $J_{\text{CP}} = 10.5$ Hz), 30, 29.9, 29.8, 29.7, 29.6, 29.5, 26.5, 22.9, 14.3; ^{31}P NMR (CDCl_3) δ 35.0, 34.9; HRMS (FAB $^+$) calcd for $\text{C}_{20}\text{H}_{39}\text{O}_6\text{PNa}$: 429.2381, found 429.2351.

(\pm)-Methyl 2-Acetyl-3-(2-(dimethoxyphosphoryl)ethyl)pentadecanoate (**16e**). To a solution of **14e** (0.33 g, 0.757 mmol) in methanol (4 mL) were added palladium on charcoal (0.08 g) and hydrogen gas to give the saturated phosphonate **16e** as a 1:1 mixture of diastereoisomers (0.33 g, 100%). Colorless oil; IR (neat, NaCl) 1736, 1712 cm^{-1} ; ^1H NMR (CDCl_3) δ 3.73 (6H, $J_{\text{HP}} = 10.8$ Hz), 3.73 (3H, app d), 3.46 (1H, d, $J_{\text{HH}} = 8.3$ Hz), 2.27 (1H, br s), 2.23 (3H, s), 1.77–1.6 (4H, m), 1.25 (20 H, br s), 0.88 (3H, t, $J_{\text{HH}} = 6.7$ Hz); ^{13}C NMR (CDCl_3) δ 203, 169.7, 63.2, 52.6 (d, $J_{\text{CP}} = 7.1$ Hz), 52.5, 38.2 (38), 32.1, 30.6 (d, $J_{\text{CP}} = 10.6$ Hz), 30, 29.9, 29.8, 29.7, 29.6, 29.5, 26.5, 22.9, 14.3; ^{31}P NMR (CDCl_3) δ 35.0, 34.9; HRMS (FAB, NBA, MH^+) calcd for $\text{C}_{22}\text{H}_{44}\text{O}_6\text{P}$: 435.2875, found 435.2868.

(\pm)-Methyl 2-Acetyl-3-(2-(dimethoxyphosphoryl)ethyl)nonadecanoate (**16f**). To a solution of **14f** (0.22 g, 0.45 mmol) in methanol (3 mL) were added palladium on charcoal (0.05 g) and hydrogen gas to give the saturated phosphonate **16f** as a 1:1 mixture of diastereoisomers (0.22 g, 100%). Colorless oil; IR (neat, NaCl) 1736, 1718 cm^{-1} ; ^1H NMR (CDCl_3) 3.72 (6H, d, $J_{\text{HP}} = 10.7$ Hz), 3.71 (3H, app d), 3.44 (1H, d, $J_{\text{HH}} = 8.9$ Hz), 2.24 (1H, br s), 2.21 (3H, s), 1.77–1.58 (4H, m), 1.23 (30H, br s), 0.86 (3H, t, $J_{\text{HH}} = 6.7$ Hz); ^{13}C NMR (CDCl_3) δ 203, 169.7, 63.1, 52.6 (d, $J_{\text{CP}} = 7.1$ Hz), 52.5, 38.3, 38, 32.1, 30.5 (d, $J_{\text{CP}} = 10.2$ Hz), 29.9, 29.7, 29.6, 29.5, 26.5, 23.5, 22.9, 20.7, 14.3; ^{31}P NMR (CDCl_3) δ 35, 34.9; HRMS (FAB, NBA, MH^+) calcd for $\text{C}_{26}\text{H}_{52}\text{O}_6\text{P}$: 491.3501, found 491.3507.

(\pm)-Methyl 2-Acetyl-3-(2-(dimethoxyphosphoryl)ethyl)henicosanoate (**16g**). To a solution of **14g** (0.28 g, 0.55 mmol) in methanol (5 mL) were added palladium on charcoal (0.06 g, 0.06 mmol) and hydrogen gas to give the saturated phosphonate **16g** as a 1:1 mixture of diastereoisomers (0.29 g, 100%). Colorless oil; IR (neat, NaCl) 1735, 1712 cm^{-1} ; ^1H NMR (CDCl_3) 3.73 (6H, d, $J_{\text{HP}} = 10.8$ Hz), 3.73 (3H, app d), 3.46 (1H, d, $J_{\text{HH}} = 8.3$ Hz), 2.26 (1H, br s), 2.23 (3H, s), 1.78–1.55 (4H, m), 1.25 (34H, br s), 0.88 (3H, t, $J_{\text{HH}} = 6.7$ Hz); ^{13}C NMR (CDCl_3) δ 203, 169.7, 63.2, 52.6 (d, $J_{\text{CP}} = 6.2$ Hz), 52.5, 38.2 (38), 32.1, 30.5, 29.9, 29.8, 29.7, 29.6, 26.5, 22.9, 14.3; ^{31}P NMR (CDCl_3) δ 35.0, 34.9; HRMS (FAB, NBA, MH^+) calcd for $\text{C}_{26}\text{H}_{57}\text{O}_6\text{PNa}$: 519.3814, found 519.3818.

General Procedure for the Synthesis of Monocyclic Phosphonate Analogs (5(α , β))–10(α , β)). To a solution of alkyl phosphonate **16** (1 mmol) in acetonitrile (2.6 mL) was added NaI (1.1 equiv), and the resulting mixture was heated at reflux. After completion of the reaction (^{31}P NMR analysis), the solvent was removed under reduced pressure to give monosodium salt as a solid. The sodium salt was suspended in methanol, Amberlite IR-120H resin (prewashed with methanol) was added, and the resulting mixture was shaken in an orbit shaker. After completion of the reaction (^{31}P NMR analysis), the resin was removed by filtration and washed with additional methanol. The solvent was removed under reduced pressure to give free monophosphonic acid as a red viscous liquid. The monophosphonic acid (1 mmol) was dissolved in freshly distilled CH_2Cl_2 (6 mL), and EDC (1.5 mmol) and HOBt (1.5 mmol) were added, followed by Hunig's base (*i*-Pr $_2$ NEt) (1.5 mmol). After the completion of the reaction (^{31}P NMR analysis), the reaction mixture was diluted with additional CH_2Cl_2 and the resulting solution was washed with saturated NaHCO_3 . The

organic layer was separated and dried over anhydrous Na_2SO_4 and then evaporated under reduced pressure to give the crude product. Purification of the crude product by chromatography (SiO_2 , 10–60% EtOAc in hexanes) gave the product as a mixture of diastereoisomers which were separated by further careful column chromatography.

(\pm)-Methyl 2-Methoxy-7-methyl-5-phenyl-2,3,4,5-tetrahydro-1,2-oxaphosphopine-6-carboxylate 2-Oxide (**5(α)** and **5(β)**). A solution of phosphonate **16b** (0.5 g, 1.46 mmol) in acetonitrile (5 mL) was treated as described above to give the monocyclic phosphonate as a 1:1 mixture of diastereoisomers (0.28 g, 52%). Further chromatographic separation of the diastereoisomers gave **5(α)** (95:5 ratio with **5(β)**). IR (neat, NaCl) 1719 cm^{-1} ; ^1H NMR (CDCl_3) δ 7.27 (m, 5H), 4.28 (1H, t, $J_{\text{HH}} = 7$ Hz), 3.86 (3H, d, $J_{\text{HP}} = 11.15$ Hz), 3.51 (3H, s), 2.25 (3H, s), 2.19 (1H, m), 2.05 (1H, m), 1.98 (1H, t, $J_{\text{HH}} = 6$ Hz); ^{13}C NMR (CDCl_3) δ 168.97, (168.78), 155.65 (d, $J_{\text{CP}} = 7.28$ Hz), (154.66); 141.35, (141.12); (129.04), 129.00; (128.10), 127.91; (127.25), 127.15; 121.44 (d, $J_{\text{CP}} = 5.1$ Hz), 53.07 (d, $J_{\text{CP}} = 6.9$ Hz), 52.71 (d, $J_{\text{CP}} = 6.9$ Hz), 52.33, 45.78 (45.63), 28.53 (d, $J_{\text{CP}} = 7.04$ Hz), 23.16 (d, $J_{\text{CP}} = 133.1$ Hz), 23.04 (d, $J_{\text{CP}} = 133.1$ Hz), 22 (21.76); ^{31}P NMR (CDCl_3) δ 30.1; HRMS (EI^+) calcd for $\text{C}_{15}\text{H}_{19}\text{O}_5\text{P}$: 310.0970, found 310.0975.

(\pm)-Methyl 2-Methoxy-7-methyl-5-pentyl-2,3,4,5-tetrahydro-1,2-oxaphosphopine-6-carboxylate 2-Oxide (**6(α)** and **6(β)**). A solution of **16c** (0.52 g, 1.55 mmol) in acetonitrile (5 mL) was treated as described above to give the monocyclic phosphonates **6** as a 1:1.25 mixture of diastereoisomers (0.27 g, 56%). Further chromatographic separation of the diastereoisomers gave **6(α)** as a pale yellow oil. IR (neat, NaCl) 1717 cm^{-1} ; ^1H NMR (CDCl_3) δ 3.82 (d, 3H, $J_{\text{HP}} = 11.18$ Hz), 3.73 (3H, s), 2.97 (1H, m), 2.22 (3H, d, $J_{\text{HH}} = 1.28$ Hz), 2.12–1.81 (4H, m), 1.61 (1H, m), 1.46 (1H, m), 1.25 (6H, br s), 0.87 (3H, t, $J_{\text{HH}} = 6.5$ Hz); ^{13}C NMR (CDCl_3) δ 169.34, 156.1 (d, $J_{\text{CP}} = 7.28$ Hz), 123.55 (d, $J_{\text{CP}} = 5.1$ Hz), 52.39 (d, $J_{\text{CP}} = 7.1$ Hz), 52.26, 37.63, 32.21, 31.1, 27.7, 25.31 (d, $J_{\text{CP}} = 6.8$ Hz), 22.93, 22.3 (d, $J_{\text{CP}} = 134.3$ Hz), 21.67, 14.44; ^{31}P NMR (CDCl_3) δ 26.8; HRMS (FAB, NBA, MH^+) calcd for $\text{C}_{14}\text{H}_{26}\text{O}_5\text{P}$: 305.1517, found 305.1523; and **6(β)** as a pale yellow oil. IR (neat, NaCl) 1717 cm^{-1} ; ^1H NMR (CDCl_3) δ 3.82 (3H, d, $J_{\text{HP}} = 11.18$ Hz), 3.75 (3H, s), 2.88 (1H, m), 2.18 (3H, d, $J_{\text{HH}} = 1.3$ Hz), 2.14–1.87 (4H, m), 1.63 (1H, m), 1.47 (1H, m), 1.25 (6H, br s), 0.87 (3H, t, $J_{\text{HH}} = 6.5$ Hz); ^{13}C NMR (CDCl_3) δ 169.51, 155.27 (d, $J_{\text{CP}} = 9.3$ Hz), 123.44 (d, $J_{\text{CP}} = 4.73$ Hz), 52.95 (d, $J_{\text{CP}} = 6.67$ Hz), 52.32, 37.5, 32.13, 31.2, 30.1, 27.65, 25.51 (d, $J_{\text{CP}} = 7.91$ Hz), 22.91, 22.64 (d, $J_{\text{CP}} = 133.33$ Hz), 21.51 (d, $J_{\text{CP}} = 1.87$ Hz), 14.43; ^{31}P NMR (CDCl_3) δ 24.2; HRMS (FAB, NBA, MH^+) calcd for $\text{C}_{14}\text{H}_{26}\text{O}_5\text{P}$: 305.1517, found 305.1523.

(\pm)-Methyl 5-Decyl-2-methoxy-7-methyl-2,3,4,5-tetrahydro-1,2-oxaphosphopine-6-carboxylate 2-Oxide (**7(α)** and **7(β)**). A solution of alkyl phosphonate **16d** (0.47 g, 1.16 mmol) in acetonitrile (3 mL) was treated as described above to give the monocyclic phosphonates **7** as a 1:1.25 mixture of diastereoisomers (0.21 g, 46%). Further chromatographic separation of the diastereoisomers gave **7(α)** as pale yellow oil. IR (neat, NaCl) 1719 cm^{-1} ; ^1H NMR (CDCl_3) δ 3.82 (3H, d, $J_{\text{HP}} = 11.2$ Hz), 3.75 (3H, s), 2.99 (1H, m), 2.23 (3H, d, $J_{\text{HH}} = 1.6$ Hz), 2.14–1.87 (4H, m), 1.62 (1H, m), 1.48 (1H, m), 1.25 (16H, br s), 0.88 (3H, t, $J_{\text{HH}} = 6.7$ Hz); ^{13}C NMR (CDCl_3) δ 169.2 (d, $J_{\text{CP}} = 1.9$ Hz), 155.9 (d, $J_{\text{CP}} = 7.3$ Hz), 123.4 (d, $J_{\text{CP}} = 5.3$ Hz), 52.2 (d, $J_{\text{CP}} = 7.1$ Hz), 52.1, 37.4, 32.1, 30.9, 29.9, 29.8, 29.7, 29.5, 27.9, 25.1 (d, $J_{\text{CP}} = 6.9$ Hz), 22.9, 22.1 (d, $J_{\text{CP}} = 134.4$ Hz), 21.51, 14.3; ^{31}P NMR (CDCl_3) δ 26.8; HRMS (FAB, NBA, MNa^+) calcd for $\text{C}_{19}\text{H}_{35}\text{O}_5\text{PNa}$: 397.2119, found 397.2125; and **7(β)** also as pale yellow oil. IR (neat, NaCl) 1719 cm^{-1} ; ^1H NMR (CDCl_3) δ 3.83 (3H, d, $J_{\text{HP}} = 11.1$ Hz), 3.76 (3H, s), 2.88 (1H, m), 2.18 (3H, d, $J_{\text{HH}} = 1.3$ Hz), 2.26–1.87 (4H, m), 1.63 (1H, m), 1.45 (1H, m), 1.25 (16H, br s), 0.88 (3H, t, $J_{\text{HH}} = 6.7$ Hz); ^{13}C NMR (CDCl_3) δ 169.3 (d, $J_{\text{CP}} = 1.7$ Hz), 155.1 (d, $J_{\text{CP}} = 9.4$ Hz), 123.3 (d, $J_{\text{CP}} = 4.6$ Hz), 52.8 (d, $J_{\text{CP}} = 6.7$ Hz), 52.1, 37.3, 32.1, 31.1, 29.9, 29.8, 29.7, 29.5, 27.8, 25.3 (d, $J_{\text{CP}} = 7.8$ Hz), 22.9, 22.5 (d, $J_{\text{CP}} = 133.4$ Hz), 21.3 (d, $J_{\text{CP}} = 1.9$ Hz), 14.3; ^{31}P NMR (CDCl_3) δ 24.2; HRMS (FAB, NBA, MH^+) calcd for $\text{C}_{19}\text{H}_{35}\text{O}_5\text{PNa}$: 397.2119, found 397.2115.

(\pm)-Methyl 5-Dodecyl-2-methoxy-7-methyl-2,3,4,5-tetrahydro-1,2-oxaphosphopine-6-carboxylate 2-Oxide (**8(α)** and **8(β)**). To a

solution of alkyl phosphonate **16e** (0.32 g, 0.74 mmol) in acetonitrile (2 mL) was treated as described above to give the monocyclic phosphonates **8** as a 1:1.25 mixture of diastereomers (0.14 g, 45%) which were further separated by column chromatography to give **8(α)** as a pale yellow oil. IR (neat, NaCl) 1719 cm⁻¹; ¹H NMR (CDCl₃) δ 3.83 (3H, d, *J*_{HP} = 11.2 Hz), 3.75 (3H, s), 2.99 (1H, m), 2.23 (3H, d, *J*_{HH} = 1.6 Hz), 2.14–1.87 (4H, m), 1.63 (1H, m), 1.47 (1H, m), 1.25 (20H, br s), 0.89 (3H, t, *J*_{HH} = 6.7 Hz); ¹³C NMR (CDCl₃) δ 169.2, 155.9 (d, *J*_{CP} = 7.1 Hz), 123.4 (d, *J*_{CP} = 5.3 Hz), 52.2 (d, *J*_{CP} = 7.8 Hz), 52.1, 37.4, 32.1, 30.9, 29.9, 29.8, 29.7, 29.6, 27.9, 25.1 (d, *J*_{CP} = 6.8 Hz), 22.9, 22.6 (d, *J*_{CP} = 134.3 Hz), 21.5, 14.3; ³¹P NMR (CDCl₃) δ 26.8; HRMS (FAB, NBA, MH⁺) calcd for C₂₁H₄₀O₅P: 403.2613, found 403.2613; and **8(β)** as pale yellow oil. IR (neat, NaCl) 1719 cm⁻¹; ¹H NMR (CDCl₃) δ 3.83 (3H, d, *J*_{HP} = 11.2 Hz), 3.76 (3H, s), 2.88 (1H, m), 2.19 (3H, d, *J*_{HH} = 1.2 Hz), 2.14–1.87 (4H, m), 1.63 (1H, m), 1.47 (1H, m), 1.25 (6H, br s), 0.87 (3H, t, *J*_{HH} = 6.5 Hz); ¹³C NMR (CDCl₃) δ 169.4, 155.1 (d, *J*_{CP} = 9.4 Hz), 123.3 (d, *J*_{CP} = 4.3 Hz), 52.8 (d, *J*_{CP} = 6.7 Hz), 52.2, 37.3, 32.1, 31.0, 29.9, 29.8, 29.7, 29.6, 27.8, 25.3 (d, *J*_{CP} = 7.7 Hz), 22.9, 22.4 (d, *J*_{CP} = 133.5 Hz), 21.3 (d, *J*_{CP} = 2.0 Hz), 14.3; ³¹P NMR (CDCl₃) δ 24.2; HRMS (FAB, NBA, MNa⁺) calcd for C₂₁H₃₉O₅PNa: 425.2439, found 425.2427.

(±)-Methyl 5-Hexadecyl-2-methoxy-7-methyl-2,3,4,5-tetrahydro-1,2-oxaphosphopine-6-carboxylate 2-Oxide (**9(α)** and **9(β)**). A solution of alkyl phosphonate **16f** (1.05 g, 2.14 mmol) in acetonitrile (5 mL) was treated as described above to give the monocyclic phosphonates **9** as a 1:1.25 mixture of diastereomers (0.45 g, 46%) which were further separated by column chromatography to give **9(α)** as a white solid. IR (neat, NaCl) 1720 cm⁻¹; ¹H NMR (CDCl₃) δ 3.82 (3H, d, *J*_{HP} = 11.2 Hz), 3.74 (3H, s), 2.98 (1H, m), 2.23 (3H, d, *J*_{HH} = 1.5 Hz), 2.14–1.88 (4H, m), 1.62 (1H, m), 1.45 (1H, m), 1.25 (30 H, br s), 0.88 (3H, t, *J*_{HH} = 6.7 Hz); ¹³C NMR (CDCl₃) δ 169.2 (d, *J*_{CP} = 1.8 Hz), 155.9 (d, *J*_{CP} = 7.3 Hz), 123.4 (d, *J*_{CP} = 5.3 Hz), 52.2 (d, *J*_{CP} = 7.1 Hz), 52.1, 37.4 (d, *J*_{CP} = 1.5 Hz), 32.1, 30.9, 30.0, 29.9, 29.8, 29.7, 29.6, 27.9, 25.1 (d, *J*_{CP} = 6.8 Hz), 22.9, 22.1 (d, *J*_{CP} = 134.4 Hz), 21.5 (d, *J*_{CP} = 1.3 Hz), 14.3; ³¹P NMR (CDCl₃) δ 26.8; HRMS (FAB, NBA, MH⁺) calcd for C₂₅H₄₈O₅P: 459.3239, found 459.3239; and **9(β)** as white solid. IR (neat, NaCl) 1720 cm⁻¹; ¹H NMR (CDCl₃) δ 3.82 (3H, d, *J*_{HP} = 11.1 Hz), 3.76 (3H, s), 2.88 (1H, m), 2.18 (3H, s), 2.11 (1H, m), 1.99 (2H, m), 1.89 (1H, m), 1.63 (1H, m), 1.49 (1H, m), 1.25 (30H, br s), 0.89 (3H, t, *J*_{HH} = 6.6 Hz); ¹³C NMR (CDCl₃) δ 169.3 (d, *J*_{CP} = 1.7 Hz), 155.1 (d, *J*_{CP} = 9.5 Hz), 123.3 (d, *J*_{CP} = 4.6 Hz), 52.8 (d, *J*_{CP} = 6.7 Hz), 52.2, 37.3, 32.1, 31.0, 30.0, 29.9, 29.8, 29.7, 29.6, 29.3, 27.8, 25.3 (d, *J*_{CP} = 7.9 Hz), 22.9, 22.4 (d, *J*_{CP} = 133.4 Hz), 21.3 (d, *J*_{CP} = 1.9 Hz), 14.3; ³¹P NMR (CDCl₃) δ 24.1; HRMS (FAB, NBA, MH⁺) calcd for C₂₅H₄₈O₅P: 459.3239, found 459.3244.

(±)-Methyl 2-Methoxy-7-methyl-5-octadecyl-2,3,4,5-tetrahydro-1,2-oxaphosphopine-6-carboxylate 2-Oxide (**10(α)** and **10(β)**). A solution of alkyl phosphonate **9g** (0.29 g, 0.56 mmol) in acetonitrile (2 mL) was treated as described above to give the monocyclic phosphonates **10** as a 1:1.25 mixture of diastereomers (0.16 g, 59%) which were further separated by column chromatography to give **10(α)** as a white solid. IR (neat, NaCl) 1719 cm⁻¹; ¹H NMR (CDCl₃) δ 3.83 (3H, d, *J*_{HP} = 11.18 Hz), 3.73 (3H, s), 2.99 (1H, m), 2.24 (3H, d, *J*_{HH} = 1.6 Hz), 2.14–1.88 (4H, m), 1.63 (1H, m), 1.47 (1H, m), 1.26 (32 H, br s), 0.89 (3H, t, *J*_{HH} = 6.7 Hz); ¹³C NMR (CDCl₃) δ 169.2, 155.9 (d, *J*_{CP} = 7.5 Hz), 123.4 (d, *J*_{CP} = 5.3 Hz), 52.2 (d, *J*_{CP} = 7.1 Hz), 52.1, 37.4, 32.1, 30.9, 30.0, 29.9, 29.8, 29.7, 27.9, 25.5 (d, *J*_{CP} = 6.9 Hz), 22.9, 22.1 (d, *J*_{CP} = 134.5 Hz), 21.5, 14.3; ³¹P NMR (CDCl₃) δ 26.8; HRMS (FAB, NBA, MH⁺) calcd for C₂₇H₅₁O₅PNa: 509.3371, found 509.3375; and **10(β)** as a white solid. IR (neat, NaCl) 1718 cm⁻¹; ¹H NMR (CDCl₃) δ 3.83 (3H, d, *J*_{HP} = 11.1 Hz), 3.76 (3H, s), 2.88 (1H, m), 2.19 (3H, d, *J*_{HH} = 1.2 Hz), 2.11 (1H, m), 2.01 (2H, m), 1.89 (1H, m), 1.64 (2H, m), 1.50 (2H, m), 1.26 (26H, br s), 0.88 (3H, t, *J*_{HH} = 6.6 Hz); ¹³C NMR (CDCl₃) δ 169.3, 155.1 (d, *J*_{CP} = 9.3 Hz), 123.3 (d, *J*_{CP} = 4.7 Hz), 52.8 (d, *J*_{CP} = 6.7 Hz), 52.2, 37.3, 32.1, 31.0, 30, 29.9, 29.7, 29.6, 27.8, 25.3 (d, *J*_{CP} = 8 Hz), 22.9, 22.4 (d, *J*_{CP} = 133.3 Hz), 21.3 (d, *J*_{CP} = 2.1 Hz), 14.3; ³¹P NMR (CDCl₃) δ 24.2; HRMS (FAB, MH⁺) calcd for C₂₇H₅₁O₅PNa: 509.3371, found 509.3363.

Methyl 7-Methyl-2-(hexadecyloxy)-2,3,4,5-tetrahydro-1,2-oxaphosphopine-6-carboxylate 2-Oxide (11). To a solution of monocyclic phosphonate analog **4** (0.024 g, 0.10 mmol) and 1-bromohexadecane (0.15 g, 0.50 mmol) in dry toluene (0.5 mL) was added *n*Bu₄Ni (TBAI) (0.003 mmol, 0.002 g, 5 mol %) at room temperature. The mixture was heated to reflux. After completion of the reaction (TLC and ³¹P NMR analysis), the solvent was removed under reduced pressure and the crude product was purified by column chromatography (SiO₂, 10–30% EtOAc in hexane) to give phosphonate analog **11** (0.037g, 86%) as a waxy solid. IR (neat, NaCl) 1717 cm⁻¹; ¹H NMR (CDCl₃) δ 4.12 (2H, m), 3.73 (3H, s), 2.65 (1H, m), 2.47 (1H, m), 2.31 (3H, s), 2.18–1.89 (4H, m), 1.68 (2H, p, *J*_{HH} = 6.9 Hz), 1.37–1.24 (26H, br s), 0.86 (3H, t, *J*_{HH} = 6.6 Hz); ¹³C NMR (CDCl₃) δ 168.22 (d, *J*_{CP} = 1.7 Hz), 159.43 (d, *J*_{CP} = 7.8 Hz), 119.20 (d, *J*_{CP} = 4.6 Hz), 66.24 (d, *J*_{CP} = 7.0 Hz), 52.00, 32.08, 30.57 (d, *J*_{CP} = 6.0 Hz), 29.85, 29.81, 29.80, 29.71, 29.66, 29.52, 27.68, 26.42, 26.78 (d, *J*_{CP} = 133.6 Hz), 26.41 (d, *J*_{CP} = 2.7 Hz), 25.61, 22.85, 21.29 21.67 (d, *J*_{CP} = 7.5 Hz), 21.12 (d, *J*_{CP} = 1.6 Hz), 14.44; ³¹P NMR (CDCl₃) δ 23.1; HRMS (FAB, NBA, MH⁺) calcd for C₂₄H₄₆O₅P: 445.3083, found 445.3076.

Methyl 7-Methyl-2-(octadecyloxy)-2,3,4,5-tetrahydro-1,2-oxaphosphopine-6-carboxylate 2-Oxide (12). The monocyclic phosphonate **4** (0.064 g, 0.26 mmol) was dissolved in dry acetone (0.5 mL), and NaI (0.044 g, 0.29 mmol) was added. The yellow solution was heated at reflux overnight. After completion of the reaction (³¹P NMR analysis) the solvent was removed under reduced pressure. The dark orange residue was dissolved in dry methanol (10 mL), and prerinced Amberlite IR-120H resin (0.320 g) was added. The mixture was shaken on an orbital shaker for 45 min, filtered, and concentrated under reduced pressure to yield a light orange oil. The oil was dissolved in dry CH₂Cl₂ (0.20 mL), and then potassium carbonate (0.040 g, 0.29 mmol) and 18-crown-6 (0.002 g, 0.08 mmol) were added, followed by the addition of *n*-octadecyl triflate (0.149 g, 0.369 mmol)⁴⁰ in dry CH₂Cl₂ (0.30 mL) dropwise. After 48 h, the reaction was quenched with deionized water and extracted three times with CH₂Cl₂. The combined organic extracts was dried over Na₂SO₄ and concentrated under reduced pressure. The crude product was purified by column chromatography (SiO₂, 7–15% EtOAc in hexanes) to give **12** (0.061 g, 49%) as a white waxy solid. IR (neat, ATR), 1712, 1646 cm⁻¹; ¹H NMR (CDCl₃) δ 4.13 (2H, m), 3.72 (3H, s), 2.65 (1H, m), 2.47 (1H, m), 2.30 (3H, s), 2.20–1.83 (4H, m), 1.67 (2H, p, *J*_{HH} = 6.8 Hz), 1.30–1.16 (28H, br s), 0.85 (3H, t, *J*_{HH} = 6.6 Hz); ¹³C NMR (CDCl₃) δ 168.19, 159.414 (d, *J*_{CP} = 7.8 Hz), 119.18 (d, *J*_{CP} = 4.6 Hz), 66.22 (d, *J*_{CP} = 7.2 Hz), 51.98, 32.07, 30.56 (d, *J*_{CP} = 6.2), 29.84, 29.81, 29.78, 29.70, 29.65, 29.51, 29.28, 26.78 (d, *J*_{CP} = 134.3 Hz), 26.39 (d, *J*_{CP} = 2.7 Hz), 25.61, 22.84, 21.33, 21.12, 14.27; ³¹P NMR (CDCl₃) δ 23.7; HRMS (FAB, NBA, MH⁺) calcd for C₂₆H₄₉O₅P: 473.3396, found 473.3385.

X-ray Structure Determination of Compound 10(α). Crystals of appropriate dimension were obtained by slow evaporation of acetone. A crystal with approximate dimensions 0.01 × 0.03 × 0.16 mm³ was mounted on a Mitgen cryoloop in a random orientation. Intensity data were collected at 150 K on a D8 goniostat at a 70 mm crystal-to-detector distance equipped with a Bruker APEXII CCD detector at Beamline 11.3.1 at the Advanced Light Source (Lawrence Berkeley National Laboratory) using synchrotron radiation tuned to λ = 1.2399 Å. For data collection, frames were measured for a duration of 1 s for low angle data and 3 s for high angle data at 0.3° intervals of ω with a maximum 2θ value of ~60°. The data frames were collected using the program APEX2 and processed using the program SAINT routine within APEX2 (Bruker Analytical X-ray, Madison, WI, 2010). The data were corrected for absorption and beam corrections based on the multiscan technique as implemented in SADABS (Bruker Analytical X-ray, Madison, WI, 2010). Crystal data and intensity data collection parameters are listed in Table 4. Structure solution and refinement were carried out using the SHELXTL-PLUS software package.⁴⁸ The structure was solved by direct methods and refined successfully in the space group P2₁/c. Full matrix least-squares refinement was carried out by minimizing Σw(F_o² - F_c²)². The non-hydrogen atoms were refined anisotropically to convergence. All hydrogen atoms were treated using

Table 4. Crystal Data and Structure Refinement for Compound 10(α)

empirical formula	C ₂₇ H ₅₁ O ₅ P	
formula weight	486.65	
temperature	150(2) K	
wavelength	1.23990 Å	
crystal system	monoclinic	
space group	P2 ₁ /c	
unit cell dimensions	$a = 10.4218(10)$ Å $b = 5.6365(5)$ Å $c = 48.570(5)$ Å	$\alpha = 90^\circ$ $\beta = 91.908(5)^\circ$ $\gamma = 90^\circ$
volume	2851.5(5) Å ³	
Z	4	
density (calculated)	1.134 Mg/m ³	
absorption coefficient	0.571 mm ⁻¹	
F(000)	1072	
crystal size	0.16 × 0.03 × 0.01 mm ³	
θ range for data collection	2.93° to 39.46°	
index ranges	$-10 \leq h \leq 10$, $-5 \leq k \leq 5$, $-49 \leq l \leq 49$	
reflections collected	111 131	
independent reflections	3094 [R(int) = 0.0813]	
completeness to $\theta = 39.46^\circ$	96.1%	
absorption correction	semiempirical from equivalents	
max and min transmission	0.9704 and 0.7626	
refinement method	full-matrix least-squares on F ²	
data/restraints/parameters	3094/47/320	
goodness-of-fit on F ²	1.105	
final R indices [I > 2 σ (I)]	R1 = 0.1522, wR2 = 0.3741	
R indices (all data)	R1 = 0.1740, wR2 = 0.3822	
largest diff. peak and hole	0.398 and -0.399 e ⁻ Å ⁻³	

the appropriate riding model (AFIX m3). Complete listings of positional and isotropic displacement coefficients for hydrogen atoms, anisotropic displacement coefficients for the non-hydrogen atoms are listed as Supporting Information (Tables S1–S5). The obtained crystal structure has been deposited at the Cambridge Crystallographic Data Centre and allocated the deposition number CCDC 873939.

In Vitro Biological Evaluation. Reagents. Orlistat, glyceryl tributyrinate (tributyrin, TC4), 1-oleoyl-rac-glycerol (1-monoolein, MC18), bovine serum albumin (BSA), sodium taurodeoxycholate (NaTDC), calcium chloride dihydrate (CaCl₂ · 2H₂O), and benzamidine, 4-morpholineethanesulfonic acid (MES) were purchased from Sigma-Aldrich-Fluka Chimie (St-Quentin-Fallavier, France). Sodium chloride (NaCl) and Tris(hydroxymethyl)aminomethane (Tris) were purchased from VWR International (Fontenay-sous-Bois, France) and from Euromedex (Mundolsheim, France), respectively. All organic solvents were purchased from Carlo Erba Reactifs-SDS (Val de Reuil, France) and were of HPLC grade. For protein digestion, trypsin of sequencing grade was purchased from Sigma-Aldrich-Fluka Chimie (St-Quentin-Fallavier, France).

Lipases. All lipolytic enzymes were produced and purified to homogeneity at our laboratory. Recombinant Human pancreatic lipase (HPL) was produced in the yeast *Pichia pastoris* and purified as described previously.⁴⁹ Recombinant guinea pig pancreatic lipase-related protein 2 (GPLRP2) was expressed in *Aspergillus oryzae* and purified as described by Hjorth et al.⁵⁰ Recombinant dog gastric lipase (DGL) was produced in transgenic maize by Meristem Therapeutics (Clermont-Ferrand, France)⁵¹ and purified as described in Roussel et al.⁴⁴ *Fusarium solani pisi* Cutinase was produced and purified according

to Lauwereys et al.⁵² The lipolytic enzymes from *Mycobacterium tuberculosis*, Rv0183 (monoglyceride lipase), and LipY (triacylglycerol lipase) were produced and purified as previously reported.^{34,53} Porcine pancreatic colipase (i.e., colipase) was purified from lipid-free porcine pancreatic powder (Laboratoire Industriel de Biologie - Soisy-sous-Montmorency, France) according to Fernandez et al.⁵⁴

Lipase Activity Measurements Using the pH-Stat Technique. Enzymatic activity was assayed at 37 °C by measuring the amount of free fatty acid (FFA) released from a mechanically stirred acylglycerol emulsion using 0.1 N NaOH with a pH-stat (Metrohm 718 STAT Titrino, Switzerland) adjusted to a fixed end point value.⁴¹ Except for Rv0183 acting on MC18 emulsions, all lipase activities were determined using TC4 specific assay emulsions: 0.5 mL of TC4 was mixed with 14.5 mL of a buffer solution. The activities of HPL were determined using the standard assay solution for pancreatic lipase:⁵⁵ 0.3 mM Tris-HCl (pH 8.0), 150 mM NaCl, 2 mM CaCl₂, and 4 mM NaTDC, in the presence of colipase added at a molar excess.⁵⁶ The assay solution for GPLRP2 was 1 mM Tris-HCl (pH 8.0), 150 mM NaCl, 5 mM CaCl₂, and 2 mM NaTDC.⁵⁰ In the case of DGL, the assay solution was 150 mM NaCl, 2 mM NaTDC, and 2 μ M BSA at pH 5.5.⁵⁷ With Cutinase, the assay solution was 2.5 mM Tris-HCl (pH 8.0), 150 mM NaCl, and 0.25 mM NaTDC. With LipY, the assay solution was 2.5 mM Tris-HCl (pH 7.5), 300 mM NaCl, and 3 mM NaTDC. With regards to Rv0183, assays were performed with 100 μ L of MC18 added to 15 mL of 2.5 mM Tris-HCl (pH 8.0), 150 mM NaCl, and 3 mM NaTDC.³⁴ All experiments were at least performed in duplicate. Activities were expressed as international units: 1 U = 1 μ mol of FFA released per minute. The specific activities of HPL, GPLRP2, DGL, Cutinase, LipY, and Rv0183, expressed in U per mg of pure enzyme, were found to be 8000 \pm 144, 2270 \pm 33, 340 \pm 21, 2270 \pm 63, 129 \pm 2, and 287 \pm 7 U/mg, respectively.

Inhibition Assays. The lipase-inhibitor preincubation method was used to test, in an aqueous medium and in the absence of substrate, the possible direct reactions between lipases and potential inhibitors.⁴¹ Each enzyme was then preincubated for 30 min at 25 °C with each inhibitor (5 mg/mL stock solution in isopropanol) at varying inhibitor molar excess ($x_1 = 2, 4, 20, 40, 100$). Experiments with HPL were performed in the presence of a 5-fold molar excess of colipase vs HPL. Lipase incubations with inhibitors were performed in the presence of 4 mM NaTDC in the case of HPL and DGL;⁵⁸ 2 mM NaTDC with GPLRP2 and Cutinase; and in the absence of NaTDC with Rv0183 and LipY. Regarding the inhibition by Orlistat, 2 mM NaTDC was used in the case of Cutinase, Rv0183, and GPLRP2. During the inhibition experiments, samples of the incubation medium were collected after a 30 min incubation period and injected into the pH-stat vessel in order to measure the residual lipase activity at varying inhibitor molar excess. The variation in the residual lipase activity was then used to determine the molar excess of the inhibitor which reduced the enzyme activity to 50% of its initial value (x_{150}).⁴² In addition, each enzyme was preincubated at 25 °C with the best inhibitor compounds, at a fixed molar excess of $x_1 = 4$ for 1 h. Then, the residual enzyme activity was measured at various times in order to determine the half-inactivation time ($t_{1/2}$).⁵⁹ The x_1 value used in these latter experiments was chosen so that the average residual activities of Cutinase, Rv0183, and LipY obtained after 30 min of incubation were in the 10–15% range. In each case, control experiments were performed in the absence of inhibitor and with the same volume of isopropanol. It is worth noting that isopropanol at a final volume of less than 5% has no effect on the enzyme activity.

The lipase stereopreference for the compounds tested was also studied on the basis of the discrimination between the two diastereoisomers *trans*-(α) and *cis*-(β) of the same compound. A Diastereoselectivity Index (DI)⁴³ was defined by eq 1:

$$DI_{(\%) } = \frac{|(x_{150})_{\beta \text{ isomer}} - (x_{150})_{\alpha \text{ isomer}}|}{(x_{150})_{\beta \text{ isomer}} + (x_{150})_{\alpha \text{ isomer}}} \times 100 \quad (1)$$

Protein Digestion Prior to MALDI-TOF Mass Spectrometry Analysis. Protein digestion was performed with sequencing grade trypsin, in line with the manufacturer's recommendations. Briefly,

samples were treated as follows: 5–50 pmol of native and inhibited protein were diluted in 15 μ L of 100 mM ammonium bicarbonate (pH 8.0) buffer and successively treated with 10 mM dithiothreitol (DTT) for 45 min at 56 °C, and 55 mM iodoacetamide (IAA) for 30 min at room temperature in the dark. Finally samples were incubated with 0.33 mg/mL trypsin solution in 25 mM ammonium bicarbonate (pH 8) buffer, and digestions were performed overnight at 37 °C. The generated peptides were then dried on a SpeedVac (10 min) and acidified with 1 μ L of 12.5% TFA in water before being analyzed by MALDI-TOF.

Matrix-Assisted Laser Desorption Ionization Time-of-Flight (MALDI-TOF) Mass Spectrometry Analysis. Cutinase, Rv0183, and LipY were preincubated for 30 min at 25 °C with compounds **4**, **7**(β), and **11** (5 mg/mL stock solution in isopropanol), respectively, at an x_1 value of 40 in order to abolish any residual lipolytic activity. In each case, blank experiments were performed in the absence of inhibitor. A saturated solution of α -cyano-4-hydroxycinnamic acid in acidified water (0.1% trifluoroacetic acid, TFA) and acetonitrile (30:70, v/v) was used as a matrix. Prior to the direct mass analysis of the entire lipases, aliquots of 1 μ L of native and inhibited lipase solutions (corresponding to 20–100 pmol of protein) were mixed with 1 μ L of a saturated solution of sinapinic acid in acidified water (0.1% TFA) and acetonitrile (60:40, v/v) and spotted onto the target. Samples were left to air-dry at room temperature. MALDI-TOF analyses were performed on a Bruker Microflex II mass spectrometer (Daltonik, Deutschland). Mass spectra were acquired in the positive ion mode, using the FlexAnalysis software program (Bruker, Daltonik, Deutschland). Protein identifications were carried out using the MASCOT version 2.2.0 search engine (Matrix Science, London, UK) and the NCBI protein database. Theoretical and experimental peptide masses were obtained using the BioTools software program (Bruker, Daltonik, Deutschland).

Molecular Docking. *In silico* molecular docking of lipase inhibitors present in the active site of lipases was performed with the Autodock Vina program.⁶⁰ The PyMOL Molecular Graphics System (version 1.3, Schrödinger, LLC) was used as the working environment with an in-house version of the AutoDock/Vina PyMOL plugin.⁶¹ The X-ray crystallographic structures of HPL, DGL, and GPLRP2 (PDB entry codes: 1LPB,⁴⁵ 1K8Q,⁴⁴ and 1GPL,²⁵ respectively) available at the Protein Data Bank were used as receptors. Docking runs were performed after replacing the catalytic serine by a glycine residue to enable the ligand (*i.e.*, the inhibitor) to adopt a suitable position corresponding to the prebound intermediate before the nucleophilic attack in the lipase active site. The box size used for the various receptors was chosen to fit the whole active site cleft and to allow nonconstructive binding positions. The model structure file was generated for each inhibitor molecule, and its geometry was refined using the Avogadro open-source program (Version 1.0.1. <http://avogadro.openmolecules.net/>).

■ ASSOCIATED CONTENT

■ Supporting Information

Supplementary Tables S1 to S5 related to X-ray structure of compound **10**(α). This material is available free of charge via the Internet at <http://pubs.acs.org>.

■ AUTHOR INFORMATION

Corresponding Author

*E-mail: jfcavalier@imm.cnrs.fr. Phone: +33 491 164 093 (J.-F. Cavalier). E-mail address: SpillingC@msx.umsl.edu; Phone: (314) 516-5437 (C. Spilling).

Author Contributions

§Both authors should be considered as equal first authors.

Notes

The authors declare no competing financial interest.

■ ACKNOWLEDGMENTS

Sadia Diomande and Vincent Delorme were funded by PhD fellowships from EGIDE and the Ministère de l'Enseignement Supérieur et de la Recherche, respectively. This work was supported by the CNRS, the Agence Nationale de la Recherche Française (ANR-07-PCVI-0009 and ANR MIEN 2009-00904 FOAMY_TUB) and by the LISA Carnot Institute (Convention ANR n°07-CARN-009-01). The compound synthesis was supported by Grant Number R01-GM076192 from the National Institute of General Medical Studies. The authors would like to thank Dr. R. Lebrun, S. Lignon, and R. Puppò (at the Proteomics platform of the Institut de Microbiologie de la Méditerranée, Marseille, France) for their precious help and support with the mass spectrometry experiments. Crystallographic data were collected through the SCrALS (Service Crystallography at Advanced Light Source) program at the Small-Crystal Crystallography Beamline 11.3.1 at the Advanced Light Source (ALS), Lawrence Berkeley National Laboratory. The ALS is supported by the U.S. Department of Energy, Office of Energy Sciences Materials Sciences Division, under Contract DE-AC02-05CH11231.

■ ABBREVIATIONS USED

AChE, acetylcholinesterase; DAG, diacylglycerol; DGL, dog gastric lipase; GPLRP2, guinea pig pancreatic lipase-related protein 2; HPL, human pancreatic lipase; HSL, hormone-sensitive lipase; MIC: minimal inhibitory concentration; MAG, monoacylglycerol; TAG, triacylglycerol; x_1 , inhibitor molar excess related to 1 mol of enzyme; x_{150} , inhibitor molar excess leading to 50% lipase inhibition

■ REFERENCES

- (1) Schmid, R. D.; Verger, R. Lipases: interfacial enzymes with attractive applications. *Angew. Chem., Int. Ed.* **1998**, *37*, 1608–1633.
- (2) Vulfson, E. Industrial applications of lipases. In *Lipases: Their Structure, Biochemistry, and Application*; Cambridge University Press: Cambridge, U.K., 1994; pp 271–288.
- (3) Lengsfeld, H.; Beaumier-Gallon, G.; Chahinian, H.; De Caro, A.; Verger, R.; Laugier, R.; Carrière, F. Physiology of Gastrointestinal Lipolysis and Therapeutic Use of Lipases and Digestive Lipase Inhibitors. In *Lipases and phospholipases in drug development*; Müller, G., Petry, S., Eds.; Wiley-VCH: Weinheim: 2004; pp 195–223.
- (4) Hadvary, P.; Sidler, W.; Meister, W.; Vetter, W.; Wolfer, H. The lipase inhibitor tetrahydrolipstatin binds covalently to the putative active site serine of pancreatic lipase. *J. Biol. Chem.* **1991**, *266*, 2021–2027.
- (5) Carrière, F.; Renou, C.; Ransac, S.; Lopez, V.; De Caro, J.; Ferrato, F.; De Caro, A.; Fleury, A.; Sanwald-Ducray, P.; Lengsfeld, H.; Beglinger, C.; Hadvary, P.; Verger, R.; Laugier, R. Inhibition of gastrointestinal lipolysis by Orlistat during digestion of test meals in healthy volunteers. *Am. J. Physiol. Gastrointest. Liver Physiol.* **2001**, *281*, G16–28.
- (6) Yang, P. Y.; Liu, K.; Ngai, M. H.; Lear, M. J.; Wenk, M. R.; Yao, S. Q. Activity-Based Proteome Profiling of Potential Cellular Targets of Orlistat - An FDA-Approved Drug with Anti-Tumor Activities. *J. Am. Chem. Soc.* **2010**, *132*, 656–666.
- (7) Du, J.; Wang, Z. Therapeutic potential of lipase inhibitor orlistat in Alzheimer's disease. *Med. Hypotheses* **2009**, *73*, 662–663.
- (8) Nelson, R. H.; Miles, J. M. The use of orlistat in the treatment of obesity, dyslipidaemia and Type 2 diabetes. *Expert Opin. Pharmacother.* **2005**, *6*, 2483–2491.
- (9) Kremer, L.; de Chastellier, C.; Dobson, G.; Gibson, K. J. C.; Bifani, P.; Balor, S.; Gorvel, J. P.; Lochet, C.; Minnikin, D. E.; Besra, G. S. Identification and structural characterization of an unusual

- mycobacterial monomeromycolyl-diacylglycerol. *Mol. Microbiol.* **2005**, *57*, 1113–1126.
- (10) Dhoubib, R.; Ducret, A.; Hubert, P.; Carriere, F.; Dukan, S.; Canaan, S. Watching intracellular lipolysis in mycobacteria using time lapse fluorescence microscopy. *Biochim. Biophys. Acta* **2011**, *1811*, 234–41.
- (11) West, N. P.; Cergol, K. M.; Xue, M.; Randall, E. J.; Britton, W. J.; Payne, R. J. Inhibitors of an essential mycobacterial cell wall lipase (Rv3802c) as tuberculosis drug leads. *Chem. Commun. (Camb.)* **2011**, *47*, 5166–8.
- (12) Hiratake, J. Enzyme inhibitors as chemical tools to study enzyme catalysis: rational design, synthesis, and applications. *Chem. Rec.* **2005**, *5*, 209–228.
- (13) Jaeger, K.-E.; Ransac, S.; Dijkstra, B. W.; Colson, C.; Vanheuveel, M.; Misset, O. Bacterial lipases. *FEMS Microbiol. Rev.* **1994**, *15*, 29–63.
- (14) Côtes, K.; Bakala N'Goma, J.; Dhoubib, R.; Douchet, I.; Maurin, D.; Carrière, F.; Canaan, S. Lipolytic enzymes in Mycobacterium tuberculosis. *Appl. Microbiol. Biotechnol.* **2008**, *78*, 741–749.
- (15) Bandyopadhyay, S.; Dutta, S.; Spilling, C. D.; Dupureur, C. M.; Rath, N. P. Synthesis and Biological Evaluation of a Phosphonate Analog of the Natural Acetyl Cholinesterase Inhibitor Cyclophostin. *J. Org. Chem.* **2008**, *73*, 8386–8391.
- (16) Dutta, S.; Malla, R. K.; Bandyopadhyay, S.; Spilling, C. D.; Dupureur, C. M. Synthesis and kinetic analysis of some phosphonate analogs of cyclophostin as inhibitors of human acetylcholinesterase. *Bioorg. Med. Chem.* **2010**, *18*, 2265–74.
- (17) Engel, R. Phosphonates as analogues of natural phosphates. *Chem. Rev.* **1977**, *77*, 349–367.
- (18) Metcalf, W. W.; van der Donk, W. A. Biosynthesis of phosphonic and phosphinic acid natural products. *Annu. Rev. Biochem.* **2009**, *78*, 65.
- (19) Cavalier, J.-F.; Buono, G.; Verger, R. Covalent inhibition of digestive lipases by chiral phosphonates. *Acc. Chem. Res.* **2000**, *33*, 579–589.
- (20) Kurokawa, T.; Suzuki, K.; Hayaoka, T.; Nakagawa, T.; Izawa, T.; Kobayashi, M.; Harada, N. Cyclophostin, acetylcholinesterase inhibitor from *Streptomyces lavendulae*. *J. Antibiot. (Tokyo)* **1993**, *46*, 1315–1318.
- (21) Malla, R. K.; Bandyopadhyay, S.; Spilling, C. D.; Dutta, S.; Dupureur, C. M. The First Total Synthesis of (±)-Cyclophostin and (±)-Cyclipostin P: Inhibitors of the Serine Hydrolases Acetyl Cholinesterase and Hormone Sensitive Lipase. *Org. Lett.* **2011**, *13*, 3094–3097.
- (22) Vertesy, L.; Beck, B.; Bronstrup, M.; Ehrlich, K.; Kurz, M.; Muller, G.; Schummer, D.; Seibert, G. Cyclipostins, novel hormone-sensitive lipase inhibitors from *Streptomyces* sp. DSM 13381. II. Isolation, structure elucidation and biological properties. *J. Antibiot. (Tokyo)* **2002**, *55*, 480–494.
- (23) Seibert, G.; Toti, L.; Wink, J. Treating mycobacterial infections with cyclipostins. WO/2008/025449.
- (24) Carrière, F.; Rogalska, E.; Cudrey, C.; Ferrato, F.; Laugier, R.; Verger, R. In vivo and in vitro studies on the stereoselective hydrolysis of tri- and diglycerides by gastric and pancreatic lipases. *Bioorg. Med. Chem.* **1997**, *5*, 429–435.
- (25) Withers-Martinez, C.; Carrière, F.; Verger, R.; Bourgeois, D.; Cambillau, C. A pancreatic lipase with a phospholipase A1 activity: crystal structure of a chimeric pancreatic lipase-related protein 2 from guinea pig. *Structure* **1996**, *4*, 1363–1374.
- (26) Thirstrup, K.; Carrière, F.; Hjorth, S.; Rasmussen, P. B.; Woldike, H.; Nielsen, P. F.; Thim, L. One-step purification and characterization of human pancreatic lipase expressed in insect cells. *FEBS Lett.* **1993**, *327*, 79–84.
- (27) Aloulou, A.; Rodriguez, J. A.; Fernandez, S.; van Oosterhout, D.; Puccinelli, D.; Carrière, F. Exploring the specific features of interfacial enzymology based on lipase studies. *Biochim. Biophys. Acta* **2006**, *1761*, 995–1013.
- (28) De Caro, J.; Sias, B.; Grandval, P.; Ferrato, F.; Halimi, H.; Carriere, F.; De Caro, A. Characterization of pancreatic lipase-related protein 2 isolated from human pancreatic juice. *Biochim. Biophys. Acta* **2004**, *1701*, 89–99.
- (29) Eydoux, C.; De Caro, J.; Ferrato, F.; Boullanger, P.; Lafont, D.; Laugier, R.; Carrière, F.; De Caro, A. Further biochemical characterization of human pancreatic lipase-related protein 2 expressed in yeast cells. *J. Lipid Res.* **2007**, *48*, 1539–1549.
- (30) Amara, S.; Lafont, D.; Fiorentino, B.; Boullanger, P.; Carrière, F.; De Caro, A. Continuous measurement of galactolipid hydrolysis by pancreatic lipolytic enzymes using the pH-stat technique and a medium chain monogalactosyl diglyceride as substrate. *Biochim. Biophys. Acta* **2009**, *1791*, 983–990.
- (31) Longhi, S.; Mannesse, M.; Verheij, H. M.; de Haas, G. H.; Egmond, M.; Knoops-Mouthuy, E.; Cambillau, C. Crystal structure of cutinase covalently inhibited by a triglyceride analogue. *Protein Sci.* **1997**, *6*, 275–286.
- (32) Egmond, M. R.; de Vlieg, J. *Fusarium solani* pisi cutinase. *Biochimie* **2000**, *82*, 1015–1021.
- (33) Parker, S. K.; Curtin, K. M.; Vasil, M. L. Purification and Characterization of Mycobacterial Phospholipase A: an Activity Associated with Mycobacterial Cutinase? *J. Bacteriol.* **2007**, *189*, 4153–4160.
- (34) Côtes, K.; Dhoubib, R.; Douchet, I.; Chahinian, H.; De Caro, A.; Carriere, F.; Canaan, S. Characterization of an exported monoglyceride lipase from Mycobacterium tuberculosis possibly involved in the metabolism of host cell membrane lipids. *Biochem. J.* **2007**, *408*, 417–427.
- (35) Saravanan, P.; Dubey, V. K.; Patra, S. Potential Selective Inhibitors against Rv0183 of Mycobacterium tuberculosis Targeting Host Lipid Metabolism. *Chem. Biol. Drug Des.* **2012**, *79*, 1056–1062.
- (36) Deb, C.; Daniel, J.; Sirakova, T.; Abomoelak, B.; Dubey, V.; Kolattukudy, P. A Novel Lipase Belonging to the Hormone-sensitive Lipase Family Induced under Starvation to Utilize Stored Triacylglycerol in Mycobacterium tuberculosis. *J. Biol. Chem.* **2006**, *281*, 3866–3875.
- (37) Mishra, K.; de Chastellier, C.; Narayana, Y.; Bifani, P.; Brown, A.; Besra, G.; Katoch, V.; Joshi, B.; Balaji, K.; Kremer, L. Functional Role of the PE Domain and Immunogenicity of the Mycobacterium tuberculosis Triacylglycerol Hydrolase LipY. *Infect. Immun.* **2008**, *76*, 127–140.
- (38) Yan, B.; Spilling, C. D. Synthesis of Cyclopentenones via Intramolecular HWE and the Palladium-Catalyzed Reactions of Allylic Hydroxy Phosphonate Derivatives. *J. Org. Chem.* **2008**, *73*, 5385–5396.
- (39) He, A.; Yan, B.; Thanavaro, A.; Spilling, C. D.; Rath, N. P. Synthesis of nonracemic allylic hydroxy phosphonates via alkene cross metathesis. *J. Org. Chem.* **2004**, *69*, 8643–8651.
- (40) Lainé, C.; Mornet, E.; Lemiègre, L.; Montier, T.; Cammas-Marion, S.; Neveu, C.; Carmoy, N.; Lehn, P.; Benvegna, T. Folate-Equipped Pegylated Archaeal Lipid Derivatives: Synthesis and Transfection Properties. *Chem.—Eur. J.* **2008**, *14*, 8330–8340.
- (41) Ransac, S.; Gargouri, Y.; Marguet, F.; Buono, G.; Beglinger, C.; Hildebrand, P.; Lengsfeld, H.; Hadváry, P.; Verger, R. Covalent inactivation of lipases. *Methods Enzymol.* **1997**, *286*, 190–231.
- (42) Ransac, S.; Rivière, C.; Gancet, C.; Verger, R.; de Haas, G. H. Competitive inhibition of lipolytic enzymes. I. A kinetic model applicable to water-insoluble competitive inhibitors. *Biochim. Biophys. Acta* **1990**, *1043*, 57–66.
- (43) Cavalier, J.-F.; Ransac, S.; Verger, R.; Buono, G. Inhibition of human gastric and pancreatic lipases by chiral alkylphosphonates. A kinetic study with 1,2-didecanoyl-*sn*-glycerol monolayer. *Chem. Phys. Lipids* **1999**, *100*, 3–31.
- (44) Roussel, A.; Miled, N.; Berti-Dupuis, L.; Riviere, M.; Spinelli, S.; Berna, P.; Gruber, V.; Verger, R.; Cambillau, C. Crystal structure of the open form of dog gastric lipase in complex with a phosphonate inhibitor. *J. Biol. Chem.* **2002**, *277*, 2266–2274.
- (45) Egloff, M.-P.; Marguet, F.; Buono, G.; Verger, R.; Cambillau, C.; van Tilbeurgh, H. The 2.46 Å resolution structure of the pancreatic lipase-colipase complex inhibited by a C₁₁ alkyl phosphonate. *Biochemistry* **1995**, *34*, 2751–2762.

- (46) Pappin, D. J. C.; Hojrup, P.; Bleasby, A. J. Rapid identification of proteins by peptide-mass fingerprinting. *Curr. Biol.* **1993**, *3*, 327–32.
- (47) Verger, R.; de Haas, G. H. Interfacial enzyme kinetics of lipolysis. *Annu. Rev. Biophys. Bioeng.* **1976**, *5*, 77–117.
- (48) Sheldrick, G. M. A short history of SHELX. *Acta Crystallogr., Sect. A* **2008**, *64*, 112–122.
- (49) Belle, V.; Fournel, A.; Woudstra, M.; Ranaldi, S.; Prieri, F.; Thome, V.; Currault, J.; Verger, R.; Guigliarelli, B.; Carriere, F. Probing the Opening of the Pancreatic Lipase Lid Using Site-Directed Spin Labeling and EPR Spectroscopy. *Biochemistry* **2007**, *46*, 2205–2214.
- (50) Hjorth, A.; Carrière, F.; Cudrey, C.; Wöldike, H.; Boel, E.; Lawson, D. M.; Ferrato, F.; Cambillau, C.; Dodson, G. G.; Thim, L.; Verger, R. A structural domain (the lid) found in pancreatic lipases is absent in the guinea pig (phospho)lipase. *Biochemistry* **1993**, *32*, 4702–4707.
- (51) Gruber, V.; Berna, P.; Arnaud, T.; Bournat, P.; Clément, C.; Mison, D.; Olgner, B.; Philippe, L.; Theisen, M.; Baudino, S. Large-scale production of a therapeutic protein in transgenic tobacco plants: effect of subcellular targeting on quality of a recombinant dog gastric lipase. *Molecular Breeding* **2001**, *7*, 329–340.
- (52) Lauwereys, M.; de Geus, P.; de Meutter, J.; Stanssens, P.; Matthyssens, G. Cloning, expression and characterization of cutinase, a fungal lipolytic enzyme. *GBF Monogr.* **1991**, *16*, 243–251.
- (53) Brust, B.; Lecoufle, M.; Tuailon, E.; Dedieu, L.; Canaan, S.; Valverde, V.; Kremer, L. Mycobacterium tuberculosis Lipolytic Enzymes as Potential Biomarkers for the Diagnosis of Active Tuberculosis. *PLoS ONE* **2011**, *6*, e25078.
- (54) Fernandez, S.; Jannin, V.; Rodier, J.-D.; Ritter, N.; Mahler, B.; Carriere, F. Comparative study on digestive lipase activities on the self emulsifying excipient Labrasol(R), medium chain glycerides and PEG esters. *Biochim. Biophys. Acta* **2007**, *1771*, 633–640.
- (55) Erlanson, C.; Borgström, B. Tributyrin as a substrate for determination of lipase activity of pancreatic juice and small intestinal content. *Scand. J. Gastroenterol.* **1970**, *5*, 293–295.
- (56) Bezzine, S.; Ferrato, F.; Ivanova, M. G.; Lopez, V.; Verger, R.; Carriere, F. Human pancreatic lipase: colipase dependence and interfacial binding of lid domain mutants. *Biochemistry* **1999**, *38*, 5499–5510.
- (57) Carrière, F.; Moreau, H.; Raphel, V.; Laugier, R.; Benicourt, C.; Junien, J. L.; Verger, R. Purification and biochemical characterization of dog gastric lipase. *Eur. J. Biochem.* **1991**, *202*, 75–83.
- (58) Marguet, F.; Cudrey, C.; Verger, R.; Buono, G. Digestive lipases: Inactivation by phosphonates. *Biochim. Biophys. Acta* **1994**, *1210*, 157–166.
- (59) Mannesse, M. L. M.; Boots, J. W. P.; Dijkman, R.; Slotboom, A. J.; Vanderhijden, H. T. W. V.; Egmond, M. R.; Verheij, H. M.; Dehaas, G. H. Phosphonate analogues of triacylglycerols are potent inhibitors of lipase. *Biochim. Biophys. Acta* **1995**, *1259*, 56–64.
- (60) Trott, O.; Olson, A. J. AutoDock Vina: Improving the speed and accuracy of docking with a new scoring function, efficient optimization, and multithreading. *J. Comput. Chem.* **2010**, *31*, 455–461.
- (61) Seeliger, D.; de Groot, B. L. Ligand docking and binding site analysis with PyMOL and Autodock/Vina. *J. Comput.-Aided Mol. Des.* **2010**, *24*, 417–22.